CHAPTER 5

Lanthanide-Macrocycle Complexes and the Targeted Detection of

Other Analytes

5.1 Introduction

Now that we have effectively demonstrated the advantages of using tailored lanthanide(macrocycle) binary complexes as highly specific, robust receptor sites, we plan to expand this receptor site design technology and apply it to the detection of other aromatic analytes. As described in Chapter 1, virtually any aromatic anion can be detected using sensitized lanthanide luminescence, provided that (1) the aryl anion can coordinate the lanthanide cation, and (2) the triplet state of the anion is well coupled to the excited state manifold of the lanthanide, though not too close as to be vulnerable to thermal deactivation. Fortunately, several flavors of aromatic ligands meet this criteria, many of which are of medical relevance. We will investigate two types in particular: salicylates and catecholamines (Figure 5.1).

Salicylates, specifically salicylurate (SU) and salicylic acid (SA), are metabolites of acetylsalicylic acid (ASA), generally known as aspirin. These metabolites are comprised of a benzene ring with a hydroxyl group adjacent to either a carboxyl group (SA) or a glycine-conjugated amide group (SU). Upon deprotonation, both form mono- or dianions that can chelate a lanthanide in a bidentate (or potentially tridentate for SU) fashion. Detection of SA using a terbium-EDTA binary complex has been previously reported,[1-3] though no methods involving lanthanides or lanthanide complexes have yet been proposed for SU.

Catecholamines, such as epinephrine (Epi), norepinephrine (NE) and dopamine (DA), are neurotransmitters involved in the 'fight-or-flight' response of the sympathetic nervous system. These hormones all contain the same *1,2*-dihydroxybenzene or catechol group, coupled to a primary or secondary ethylamine group on the opposite side of the

aryl ring. The protonation constants of the two phenol hydrogens tend to have a large gap, with the first pK_a starting around 8.5 and the other approaching 13 or greater.[4, 5] We will therefore explore chelation of these species to lanthanide-macrocycle complexes in extremely basic conditions to allow for bidentate coordination to the lanthanide.

Due to time constraints or difficulties with certain analytes (extreme pH conditions, light-sensitivity, solubility problems, etc.) most of these investigations are incomplete. We consequently present this work not as a comprehensive study, but rather as a collection of 'first-steps' in the endeavor to engineer selective, robust lanthanide receptor sites for the targeted detection of aryl analytes of interest.

5.2 Salicyluric Acid

5.2.1 Introduction

Acetylsalicylic acid, commonly known as aspirin, is one of the most widely used therapeutic substances. Aspirin is effective as an anti-inflammatory agent, an analgesic to relieve minor aches and pains, and an antipyretic to reduce fever.[6] It is also the primary medication used to treat chronic rheumatic fever, rheumatoid arthritis and osteoarthritis.[7] Further, recent studies have shown the anti-thrombotic benefits of an aspirin regimen in stroke prevention.[8, 9] The widespread use of aspirin mandates a complete and thorough understanding of the pharmacodynamics and pharmacokinetics of this medication in the human body. In addition, salicylates are used as markers to assess free radical damage *in vivo* due to hydroxyl radicals.[10] As a result, a detection method to monitor acetylsalicylate and its metabolites in blood plasma and urine – with high sensitivity at low cost – is in high demand.

In the body, acetylsalicylic acid (ASA) is hydrolyzed to salicylic acid (SA) by carboxylesterases in the gut walls and liver, with an elimination half-life of 15–20 minutes.[11] Salicylic acid is then metabolically converted primarily to salicyluric acid (SU) and other metabolites, which are excreted in the urine.[12, 13] Due to the high elimination rate constant for SU in comparison to SA,[14] and the fact that endogenous SU formation only occurs in a limited capacity,[15, 16] it is possible to use SU urinary excretion data to establish a relationship between SU formation and the amount of SA in the body. We can therefore use SU as an indicator of SA in vivo, and hence detection of SU in urine can be utilized as a noninvasive means of monitoring aspirin dosage and residence in the body. Further, unusually high or low concentrations of SU in the urine have been correlated to a variety of diseases and conditions, such as appendicitis, anemia, abdominal trauma, liver diseases, uremia and Down's Syndrome.[17] Hence, detection of SU in urine has a variety of applications, including a facile way to monitor aspirin dosage and corroborating the presence of certain medical conditions.

Current detection methods of salicylates in blood and urine involve significant sample preparation prior to analysis and are time- and/or labor-intensive. High performance liquid chromatography (HPLC) can be used to detect ASA, SA and SU simultaneously with a sensitivity of 0.1 mg/L,[18] but this requires solvent extraction and the addition of internal standards. Other HPLC techniques report sensitivities of 0.2 mg/L SA in urine[12] or 0.5 mg/L SA in plasma.[19] A liquid chromatographic method with UV detection has a sensitivity of 0.5 mg/L with a precision of 8.6 mg/L, but takes 25 minutes and requires purification steps.[20] Capillary electrophoresis coupled to laser-induced fluorescence has also been described to detect SA, SU and other metabolites in

urine following sample filtration and dilution.[21] A spectrophotometric method using absorption spectra and multicomponent analysis can distinguish between SA and SU, but not in blood or urine.[22] We therefore seek a method with similar sensitivity but greater efficiency that is cost-effective.

Salicylurate has been shown to bind metal cations such as divalent copper,[23] trivalent cobalt,[24] VO(IV)[25] and dimethyltin(IV).[26] In such complexes SU is either bidentate or tridentate, coordinating through the carbonyl, carboxyl and phenolate oxygens of the ligand. Lanthanides as hard ions make excellent chelators for oxygen-containing ligands. However, no lanthanide complexes containing ligated SU have been reported in the literature. Europium-macrocycle complexes have previously been applied to the detection of oxyanions in urine such as lactate and citrate.[27, 28] Here, we report the first lanthanide-macrocycle receptor to detect salicylurate in urine.

We have selected the Tb(DO2A)$^+$ binary complex, where DO2A is the macrocyclic ligand *1,4,7,10*-tetraazacyclododecane-*1,7*-bisacetate, as our first-generation salicylurate receptor site. Terbium is the only luminescent lanthanide with a solitary excited state ($^5D_4$, 20,500 cm^{-1})[29] lying below the triplet excited state of salicylate (23,000 cm^{-1}),[30] which is responsible for sensitization via energy transfer to the lanthanide.[31] Europium, dysprosium and samarium all have at least two excited state energy levels below the chromophore triplet, which results in multiple nonradiative deactivation pathways and decreased luminescence intensity.[32-34] Terbium also has a large energy gap between the lowest lying excited state and the ^7F_n ground state manifold, allowing for intense emission in the visible region (λ_{max} = 544 nm).[29] The DO2A ligand binds Tb^{3+} with high affinity (log K_{GdDO2A} = 19.4 [35]), conferring thermo-

dynamic stability and reducing vibrational quenching of luminescence by excluding solvent molecules from the lanthanide coordination sphere. Further, our work with the dipicolinate system indicates that terbium exhibits the greatest perturbation of electron density due to the electron-withdrawing effects of a chelating ligand (Section 3.7), and therefore the Tb(DO2A)$^+$ complex presents a binding site with the greatest attraction to an anionic analyte. We consequently expect coordination of the salicylurate anion to produce a strongly luminescent Tb(DO2A)(SU)$^-$ ternary complex. This work demonstrates a proof-of-concept in terms of designing a lanthanide-based receptor site to monitor medication dosage in a manner that is rapid and cost-effective.

5.2.2   Spectroscopy and Characterization

Experimental Section

Materials.   The following chemicals were purchased and used as received: ammonium hydroxide (NH$_4$OH 28–30% in water) (Mallinckrodt Baker), ether anhydrous (Acros Organics), sodium hydroxide (NaOH 50% in water) (Mallinckrodt Baker), TAPS (*N*-tris(hydroxymethyl)methyl-*3*-aminopropanesulfonic acid) buffer (TCI America), trifluoroacetic acid (*2,2,2*-trifluoroacetic acid, TFA) (J. T. Baker), terbium(III) chloride hexahydrate (Alfa Aesar), and SU (salicyluric acid, *2*-hydroxyhippuric acid) (Acros Organics). The TbCl$_3$ salt was 99% pure, all solvents were ACS certified or HPLC grade, all buffers were at least 98% pure, and SU was 97% pure. Water was deionized to a resistivity of 18.2 MΩ-cm using a Purelab® Ultra laboratory water purification system (Siemens Water Technologies, Warrendale, PA). The *1,4,7,10*-tetraazacyclododecane-*1,7*-diacetate (DO2A) ligand was prepared by hydrolysis of *1,4,7,10*-tetraazacyclo-

dodecane-*1,7*-di(tert-butyl acetate) (Macrocyclics, Dallas, TX), as described previously (Section 2.2.1) resulting in a white solid in 79.9% yield. DO2A·0.6H₂O·2.1HCl. Anal. Calcd. (found) for $C_{12}H_{24}N_4O_4$ ·2.80HCl · 0.85H₂O (fw = 378.18): C, 38.32 (38.32); H, 7.31 (7.19); N, 14.89 (14.54); Cl, 20.0 (20.0).

The *1,4,7,10*-tetraazacyclododecane-*1,4,7*-triacetate (DO3A) ligand was prepared by hydrolysis of *1,4,7,10*-tetraazacyclododecane-*1,4,7*-tri(*t*-butyl-acetate)·HBr (DO3A-tBu-ester) (Macrocyclics) with trifluoroacetic acid (TFA).[36] All glassware used in this procedure was washed, placed in a nitric acid digest (50% HNO_3 in nanopure water), rinsed 10 times with nanopure water and kilned at 500 °C for 2 hours prior to use. The DO3A-tBu-ester HBr salt (2.50060 g, 4.198 mmol), a white powder, was placed in a 100-mL cylindrical flask with a side inlet and top opening fitted with a glass stopper. Neat TFA (10.0 mL, 134.6 mmol) was added at room temperature to produce a clear yellow solution. This solution was left stirring at room temperature open to air (side inlet cracked slightly) for 22 hours. The TFA was removed by rotary evaporation under vacuum (~ 50 mbar) in a hot water bath (55 °C) leaving a yellow oil. White crystals were obtained after 8 days at room temperature. The product was rinsed with two 10-mL aliquots of ether using a new fine frit (Pyrex, 15 mL, ASTM 4-5.5F, No. 36060) and dried by pulling air through the sample for 15 minutes to produce a white powder of DO3A·1.9H₂O·3.0TFA (2.50298 g, 3.486 mmol) in 83.05% yield. Anal. Calcd (found) in duplicate for $C_{14}H_{27}N_4O_6$·1.9H₂O·3.0C₂HF₃O₂ (fw = 717.96): C, 33.42 (33.43); H, 4.18 (4.27); N, 7.80 (7.93). ESI-MS (*m/z*): calcd (found) for $C_{14}H_{27}N_4O_6$ (M + H): 347.1931 (347.1939). ^{13}C NMR: δ 42.18, δ 47.62, δ 49.07, δ 51.83, δ 52.97, δ 55.02, δ 115.08, δ 163.02, δ 168.96, δ 174.32.

The Tb(DO2A)(SU)$^-$ ternary complex was prepared in aqueous solution by addition of 0.464 mL of 0.032318 M TbCl$_3$ (15.00 μmol) to 0.269 mL of 0.5593 M DO2A (15.05 μmol), followed by 1.650 mL of 9.0717 mM SU (14.97 μmol). pH was adjusted to 8.0 with ammonium hydroxide (28–30% in H$_2$O), added dropwise. TOF-MS ES$^-$ (*m/z*): calcd (found) for TbC$_{21}$H$_{29}$N$_5$O$_8$ (M$^-$): 638.41 (638.13).

Methods. All samples were prepared in triplicate to a final volume of 3.50 mL in disposable acrylate cuvettes (Spectrocell, Oreland, PA) with a 1 cm path length. Luminescence spectral analysis was performed by a Fluorolog Fluorescence Spectrometer (Horiba Jobin-Yvon, Edison, NJ). To prevent second-order diffraction of the source radiation, all measurements were taken with a 350-nm colorless sharp cutoff glass filter (03 FCG 055, Melles Griot, Covina, CA). All reported spectra were obtained as a ratio of corrected signal to corrected reference (S$_c$/R$_c$) to eliminate the effect of varying background radiation in the sample chamber; emission intensities are in units of counts per second per microampere (cps/μA).

Luminescence excitation (λ_{ex} = 316 nm) and emission (λ_{em} = 544 nm) spectra were obtained for the Tb(macrocycle)(SU) ternary complexes, where the macrocycle was DO2A or DO3A, at a concentration of 100 μM in 0.1 M TAPS buffer, pH 8.4. Absorption spectra were obtained using a Cary 50 Bio UV/visible spectrophotometer (Varian, Inc., Palo Alto, CA) in quartz cuvettes.

Several attempts were made to crystallize the Tb(DO2A)(SU)$^-$ ternary complex out of acetone with a tetrabutylammonium counterion. However, the only crystals obtained were of a trimer containing terbium and the macrocycle, but no salicylurate. We believe this is due to the low to moderate stability of the ternary complex.

Results and Discussion

The excitation spectrum of the Tb(DO2A)(SU)$^-$ complex shows a broad band at 316 nm, attributed to the $\pi \rightarrow \pi^*$ transition of the SU chromophore.[37] The emission spectrum presents a large, broad band with a λ_{max} of 419 nm, presumably due to excited state intramolecular proton transfer (ESIPT) from the hydroxyl moiety to the nearby carbonyl group of the SU ligand. This type of ESIPT is known to occur in salicylic acid and para-methoxy substituted salicylates, with similar excitation and emission wavelengths.[38, 39] The unusually large Stokes shifts in these compounds are due to a significant geometry change as the proton-transfer tautomer is formed and then relaxes to a relatively unstable isomer of the ground state.[40-42] This band at 419 nm can be used as an internal standard to validate SU concentration in solution (Figure 5.2).

The sharp bands at 488, 545, 585 and 621 nm are the $^5D_4 \rightarrow {}^7F_n$ transitions for sensitized terbium emission, where n = 6,5,4 and 3, respectively (Figure 5.3). The intensities of these transitions are consistent with the luminescence turn-on associated with an aromatic anion binding to the terbium cation and yielding efficient intersystem crossing via the absorption-energy transfer-emission (AETE) mechanism following UV excitation. This effect results in an increase in terbium luminescence by several orders of magnitude, and cannot be accounted for simply by the exclusion of water – which quenches luminescence via nonradiative decay pathways – from the Tb^{3+} coordination sphere.[43, 44]

The ESIPT band at 419 nm can also provide information concerning the coordination behavior of the salicylurate ligand. Though our luminescence measurements were made at pH 8.4, above the two pK_a values of SU (Table 5.1),[23] we

still see strong evidence of intramolecular proton transfer, indicating that the phenol moiety of the SU is still protonated. If this is the case, then the terbium would interfere with proton transfer if it were coordinating to the carbonyl and phenolate groups as expected. Most likely, the SU is binding to the lanthanide in a bidentate fashion via the carbonyl and the carboxyl group (Figure 5.4). However, a tridentate motif involving the amine group is also a possibility. The excitation and emission spectra of the Tb(DO3A)(SU)$^{2-}$ complex are more than an order of magnitude lower in intensity than the corresponding DO2A spectra (Figure 5.5), indicating that the SU ligand does not bind with much affinity to the Tb(DO3A) complex. This may corroborate either the tridentate chelation motif or a bidentate mode with a significant amount of steric bulk around the binding site, as apparently two adjacent binding sites on the lanthanide are not sufficient for SU ligation. Only the Tb(DO2A)$^{+}$ complex, which has three linear adjacent binding sites available on the Tb^{3+} cation, is able to accommodate the SU ligand.

5.2.3   Binding Studies and Stability

Experimental Section

Materials.   The following chemicals were purchased and used as received: CAPS (*N*-cyclohexyl-3-aminopropanesulfonic acid) buffer (Alfa Aesar), CHES (*N*-cyclohexyl-*2*-aminoethanesulfonic acid) buffer (Alfa Aesar), MES monohydrate (*2*-(*N*-morpholino) ethanesulfonic acid monohydrate) buffer (Alfa Aesar), sodium acetate trihydrate (Mallinckrodt), sodium hydroxide (NaOH 50% in water) (Mallinckrodt Baker), TAPS (*N*-tris(hydroxymethyl)methyl-*3*-aminopropanesulfonic acid) buffer (TCI America), terbium(III) chloride hexahydrate (Alfa Aesar) and SU (salicyluric acid, *2*-

hydroxyhippuric acid) (Acros Organics). The $TbCl_3$ salt was 99% pure, all buffers were at least 98% pure and SU was 97% pure. DO2A was prepared as previously described (Section 2.2.1). Water was deionized to a resistivity of 18.2 MΩ-cm using a Purelab® Ultra laboratory water purification system.

Methods. All samples were prepared in triplicate to a final volume of 3.50 mL in disposable acrylate cuvettes (Spectrocell) with a 1 cm path length. Luminescence spectral analysis was performed by a Fluorolog Fluorescence Spectrometer with a 350-nm colorless sharp cutoff glass filter as previously described (Section 5.2.2). Integrated intensities are evaluated over 534–554 nm. The solution pH was measured using a calibrated handheld IQ150 pH/mV/temperature meter (I. Q. Scientific Instruments, Loveland, CO) following data collection. Because of SU intrinsic luminescence, all integration values are reported after emission spectra are fit and then subtracted to a SU aqueous solution to isolate the bound Tb-SU signal.

Binding studies. A method of continuous variations was used to determine the binding stoichiometry for the Tb/DO2A/SU system. Samples were prepared in 0.1 M TAPS buffer (pH 8.4) with the concentrations of Tb and SU varying inversely from 0 to 120 μM in 10 μM increments, and the concentration of DO2A maintained at 500 μM. Emission spectra were obtained following 1–3 hours of equilibration time.

pH dependence study. Solutions of 100 μM Tb(DO2A)(SU)⁻ were prepared in 0.1 M buffer with five-fold excess DO2A to ensure full Tb complexation. Four buffers were used: MES (pK_a = 6.1), TAPS (pK_a = 8.4), CHES (pK_a = 9.3) and CAPS (pK_a = 10.4), with pH adjustment to within 0.1 of the pK_a value using 50% NaOH added dropwise.

Sodium acetate trihydrate, 0.2 M, was also used to maintain a pH of 7.5. Emission spectra were obtained after 15 min, 18 hrs and 5 days.

Results and Discussion

A method of continuous variations indicates an optimal binding stoichiometry of about 1:1 for Tb and SU with DO2A in excess (Figure 5.6). We can therefore conclude that SU^{2-} binds to $Tb(DO2A)^+$ to form the $Tb(DO2A)(SU)^-$ complex. However, the curvature of the Jobs plot may indicate lower stability than anticipated of the ternary complex. This can be mitigated by working in a higher concentration regime.

To optimize conditions for detection of SU in complex matrices, a pH dependence study was performed from pH 6.1 to 10.6. Results indicate that the $Tb(DO2A)(SU)^-$ complex is most stable in neutral to slightly basic conditions, with pH 8.4 optimal (Figure 5.7). This is consistent with the pK_a values reported for SU (3.34 and 7.91)[23] suggesting that the SU ligand must be at least partially deprotonated for effective terbium binding and efficient energy transfer. Experiments indicate that the $Tb(DO2A)(SU)^-$ complex is unstable after 24 hours, as evidenced by a significant loss of signal. Reproducibility is conserved if samples are analyzed within 5–6 hours of solution preparation.

5.2.4   Calibration Curve and Limit of Detection

Experimental Section

Materials.   The following chemicals were purchased and used as received: TAPS (*N*-tris(hydroxymethyl) methyl-*3*-aminopropanesulfonic acid) buffer (TCI America), terbium(III) chloride hexahydrate (Alfa Aesar) and SU (salicyluric acid, *2*-

hydroxyhippuric acid) (Acros Organics). DO2A was prepared as previously described (Section 2.2.1). Water was deionized to a resistivity of 18.2 MΩ-cm using a Purelab® Ultra laboratory water purification system. Urine was collected from healthy volunteers, with unmarked samples chosen at random from a larger sample set for analysis within 24 hours of donation. Samples were kept refrigerated at 4 °C until use.

Methods. All samples were prepared in triplicate to a final volume of 3.50 mL in disposable acrylate cuvettes (Spectrocell) with a 1 cm path length. Luminescence spectral analysis was performed by a Fluorolog Fluorescence Spectrometer with a 350-nm colorless sharp cutoff glass filter as previously described (Section 5.2.2).

Urine samples were spiked with SU over a range from 0–150 μM. An aliquot from each spiked sample was diluted into a pre-equilibrated solution containing 5 mM Tb(DO2A)$^+$ in 0.1 M TAPS buffer (pH 8.4) in various volumes, and the emission spectra obtained within 1 hour of dilution. Intrinsic SU fluorescence was eliminated from the emission spectra using a fitting algorithm, and the largest terbium emission peak at 544 nm was integrated and normalized to an external standard. A linear regression model was used to determine the endogenous SU concentration in each donated sample by setting the y-intercept to the integrated intensity of 5 mM Tb(DO2A)$^+$ alone (I_0), and solving for an endogenous SU concentration $[SU]_{end}$ such that the correlation coefficient (R^2) is optimized to near unity (equation 5.1).

$$I_{obs} = C \cdot \left([SU]_{spike} + [SU]_{end} \right) + I_0$$

[5.1]

In this model, I_{obs} is the observed integrated intensity of the spiked sample in 5 mM Tb(DO2A)$^+$, $[SU]_{spike}$ is the concentration of SU added to the sample, and *C* is the calibration constant, in units of cps/(M·μA). It was empirically determined from these

experiments that a sample dilution factor of 1:350 produces a linear, reproducible correlation between SU concentration and emission intensity that is independent of donor. A calibration curve was generated from this data set, and can be applied to any urine sample to determine SU concentration.

The limit of detection (LOD) for SU in urine was identified for a signal to noise ratio of 3:1. An average noise value was obtained from an emission spectrum used in the calibration curve (λ_{em} = 544 nm); this was multiplied by the S/N ratio and added to the background intensity (λ_{em} = 542 nm) for a 5 mM Tb(DO2A)$^+$ control solution. Integration of the Tb(DO2A)(SU) emission spectrum adjusted to this value resulted in an SU concentration obtained from the constructed calibration curve that corresponds to the limit of detection for this assay.

Results and Discussion

To determine the efficacy of SU detection using the Tb(DO2A)$^+$ receptor site in body fluids, urine samples provided by healthy donors were used to generate a calibration curve and calculated a limit of detection. Signal quenching was observed with high concentrations of urine, probably due to competition with other ions or loss of emission signal due to the high absorptivity of the samples. Dilution of the sample while maintaining a high concentration of Tb(DO2A)$^+$ (4–5 mM) eliminated this problem and produced results similar to those obtained in aqueous solution (Figure 5.8). A dilution factor of 1:350 allows for reproducibility over the entire sample set tested. Using this dilution factor, a calibration curve was constructed using spiked SU urine samples from three separate donors, with a correlation coefficient near unity (Figure 5.9). Assuming a

signal-to-noise ratio of 3:1, a limit of detection (LOD) for this assay was determined to be 0.027 μM SU in the diluted samples, which corresponds to an SU concentration of 9.4 μM in urine or approximately 1.8 mg/L. For a first iteration of an SU receptor site, this value is already in the range of highly specialized detection methods such as HPLC or capillary electrophoresis, and can be performed in a fraction of the time.

5.2.5   Aspirin Study

<u>Experimental Section</u>

Materials. TAPS (*N*-tris(hydroxymethyl) methyl-*3*-aminopropanesulfonic acid) buffer (TCI America, Portland, OR) and terbium(III) chloride hexahydrate (Alfa Aesar) were purchased and used as received. DO2A was prepared as previously described (Section 2.2.1). Water was deionized to a resistivity of 18.2 MΩ-cm using a Purelab® Ultra laboratory water purification system. Urine collected from a healthy anonymous volunteer was kept refrigerated at 4 °C until use.

Methods. All samples were prepared in triplicate to a final volume of 3.50 mL in disposable acrylate cuvettes (Spectrocell) with a 1 cm path length. Luminescence spectral analysis was performed by a Fluorolog Fluorescence Spectrometer with a 350-nm colorless sharp cutoff glass filter as previously described (Section 5.2.2).

Samples were collected from a healthy anonymous volunteer before and following two self-medicated aspirin regimens. The subject took 81 mg of aspirin every 6 hours for a total of 24 hours, and provided a urine sample 4 hours after the final dose. The process was repeated again with a 325-mg regimen. Both regimens were within recommended low-dose ranges for stroke and myocardial infarction prevention.[8] A 10-

µL aliquot of each sample was diluted 1:350 into pre-equilibrated 5.0 mM Tb(DO2A)$^+$ in 0.1 M TAPS (pH 8.4). Emission spectra (λ_{ex} = 316 nm) were obtained following 1 minute of thorough mixing.

Results and Discussion

As a proof-of-concept, we obtained urine samples from a healthy anonymous volunteer on a low-dose aspirin regimen. We successfully detected an increase in luminescence intensity that tracked with the two aspirin dosage aliquots of 81 mg or 325 mg, indicating an increase in SU elimination in the urine (Figure 5.10). The intensity of the intrinsic SU luminescence band (419 nm) is much lower relative to the terbium emission peaks for this experiment. We attribute the decrease to absorption by other species in solution in this region. The unpredictable change in intensity of this band, which varies significantly between donors, emphasizes the problems associated with using SU luminescence alone for concentration determination and reinforces our technique of using sensitized lanthanide luminescence that is specific for SU.

5.2.6   Conclusion

We have demonstrated a first-generation SU receptor site composed of a lanthanide reporter chelated to a selective macrocyclic ligand. Preliminary results suggest a high degree of selectivity for SU, even in a matrix as complex as urine. Complete sample preparation and analysis can be performed within 5 minutes. This SU detection assay represents a proof-of-concept for the design and implementation of lanthanide-macrocycle receptor sites with high sensitivity and selectivity for a target

biomolecule. Further optimization of the macrocycle by adding or substituting functional groups to modify the electrostatics and sterics of the Tb receptor site should enhance SU binding and improve the limit of detection by at least an order of magnitude.[45] Such an improvement would make this type of SU detection more sensitive than all other reported techniques, in addition to being more rapid and cost-effective.

Spectroscopic determination of salicylurate by terbium-macrocycle complexes has three advantages: (1) rapid detection and quantification, (2) low cost and (3) capability of automation. We anticipate application of such a straightforward method for in-line monitoring of SU, possibly via an automated cathaderized system. Salicylurate levels in the bloodstream could also be determined using sufficiently selective terbium complexes, though further experimentation is required.

5.3   Salicylic Acid

5.3.1   Introduction

Salicylic acid, named after the willow tree (*Salix* genus) from whose leaves and bark it was originally obtained, is the primary metabolite of aspirin. As stated in Section 5.2.1, acetylsalicylic acid (ASA) of aspirin is rapidly hydrolyzed upon ingestion to salicylic acid (SA), which is later converted to salicylurate (SU) and other compounds. Salicylic acid itself also has many applications due to its keratinolytic effects and ability to affect metabolic processes;[46] common uses include food preservation, acne medication and topical treatment of fungal skin infections.[47, 48] Further, SA sensitivity can cause ototoxicity (hearing loss) and metabolic acidosis in some individuals.[49, 50]

Salicylic acid can be toxic when taken in large doses.[51]   The recommended therapeutic level in plasma is around 150–300 mg/L. SA intoxication symptoms can start to appear at 300 mg/L plasma concentration, and severe intoxication, including acidosis and tetany (involuntary muscle contraction) can occur at levels above 500 mg/L.[52] Many methods for the detection of salicylic acid have been reported, including colorimetric,[53] fluorimetric,[54, 55] chromatographic[20, 56-58] and voltametric[59] assays. The simplest and most cost-effective method is the Trinder test, in which salicylate binds to Fe^{3+} to produce a purple complex which can be quantified by optical density (530 nm).[60] However, this technique suffers from poor selectivity and false positives.[61]

As described in Section 5.2.1, current methods of detection for salicylates are too slow, too expensive, or have poor detection limits. Additionally, most involve sample pretreatment, such as extraction, derivatization or preconcentration steps prior to analysis. Salicylate can form chelate compounds with metal ions, with most stability constants in the micromolar range (log K = 5.5 to 7.0) in near-neutral conditions; the notable exceptions are Cu^{2+} (log K = 10.6) and Fe^{3+} (log K = 16.4).[62] This propensity to effectively bind divalent and trivalent ions makes salicylic acid an ideal candidate for detection methods involving complexation to lanthanides. The triplet excited state of salicylic acid $(23,041 \text{ cm}^{-1})$[30] lies in the optimal energy transfer region to effectively sensitize the terbium cation $(20,500 \text{ cm}^{-1})$.[29] As a result, assays involving SA detection in serum using the Tb(EDTA) binary complex have been proposed, with limits of detection in the micromolar range at high pH.[2, 3] These involve second derivative scanning fluorescence spectrometry or purification using capillary electrophoresis.   Another

method involving micelles claims a subnanomolar detection limit, although this was for pure salicylic acid in buffered aqueous solution.[1]

Due to the kinetic and thermodynamic stability of macrocyclic ligands and our previous success in receptor site design involving lanthanide-macrocycle complexes, we plan to explore cyclic chelating ligands in the detection of SA and compare these to results obtained with EDTA. A neutral terbium complex of a DO3A derivative with a pendant 15-aza-crown-5 substituent has also been found to chelate salicylic acid with a binding affinity in the millimolar range (log K_a' = 3.9 ± 0.2) in 0.1 M Tris buffer, pH 7.4.[63] We believe we can substantially enhance the binding affinity for salicylate with judicial choice of chelating macrocycle and shifting the pH to more basic conditions where the salicylate is fully deprotonated (Table 5.1).[64, 65] We will use a screening protocol to determine the optimal chelating ligand, whether cyclic or acyclic, that when combined with terbium produces the most effective receptor site for salicylate.

5.3.2   Photophysics and Ligand Screen

As with the salicylurate system (Section 5.2) the photophysics of salicylate are more complex, owing to the phenomenon of excited-state intramolecular proton transfer (ESIPT) from the phenol to the proximal carboxyl moiety during tautomerization of the photoexcited SA structure.[38-40, 42] We will explore the effect of lanthanide chelation on the intrinsic luminescence of salicylic acid.

Several macrocyclic ligands of varying denticity (hexa- to octadentate) will be used to generate Tb(ligand)(SA) ternary complexes in highly basic conditions. The screening protocol will involve obtaining excitation and emission spectra; the optimal SA

receptor site complex should produce the greatest luminescence intensity for a given concentration. Salicylic acid is also light-sensitive, so a photodegradation study will be performed as well.

Experimental Section

Materials. The following chemicals were purchased and used as received: CAPS (*N*-cyclohexyl-*3*-aminopropanesulfonic acid) buffer (Alfa Aesar), CHES (*N*-cyclo-hexyl-*2*-aminoethanesulfonic acid) buffer (Alfa Aesar), DOTA (*1,4,7,10*-tetraazacyclo-dodecane-*1,4,7,10*-tetraacetate) (Macrocyclics), EDTA (ethylenediaminetetraacetic acid) (Aldrich), sodium hydroxide (NaOH 50% in water) (Mallinckrodt Baker), sodium salicylate (NaSA, sodium *2*-hydroxybenzoic acid) (Fisher) and terbium(III) chloride hexahydrate (Alfa Aesar). All lanthanide salts were 99.9% pure and all other salts were 97% pure or greater. Water was deionized to a resistivity of 18.2 MΩ-cm using a Purelab® Ultra laboratory water purification system. DO2A was prepared as previously described (Section 2.2.1). DO3A was prepared as previously described (Section 5.2.2).

Methods. All samples were prepared in triplicate *under a red light* from stock solutions to a final volume of 4.00 mL in disposable acrylate cuvettes (Spectrocell) with a 1 cm path length and *stored in the dark* at room temperature prior to analysis. Luminescence spectral analysis was performed by a Fluorolog Fluorescence Spectrometer with a 350-nm cutoff filter as previously described (Section 5.2.2). The solution pH was measured using a calibrated handheld IQ150 pH/mV/temperature meter (I. Q. Scientific Instruments).

Spectroscopy.   Cuvettes of 10.0 µM SA, Tb(SA) and Tb(ligand)(SA), where ligand is EDTA, DO3A or DOTA, were prepared in 0.1 M MOPS buffer (pH 7.5) and 0.1 M CAPS buffer (pH 10.0).   All Tb(ligand) complexes were pre-equilibrated for at least 2 weeks prior to use.   Absorbance measurements were made using a Cary 50 Bio UV/Visible Spectrophotometer (Varian, Inc., Palo Alto, CA) following 1 hour equilibration time.   Excitation (λ_{em} = 544 nm) and emission (λ_{ex} = 314 nm) spectra were also obtained following 1 hour of equlibration.

Ligand screen study.   Cuvettes of 1.0 µM SA and either 100 µM or 1.0 mM of Tb(ligand), where ligand is EDTA, DO2A, DO3A or DOTA, were prepared in 50 mM CAPS or CHES (DO2A only) buffer, pH 12.5.   All Tb(ligand) complexes were pre-equilibrated for at least 2 weeks prior to use.   Excitation (λ_{em} = 544 nm) and emission (λ_{ex} = 326 nm) spectra were obtained following 1, 2, 3, 4, 8, 24, 48 and 72 hours equilibration time.

Photodegradation study.   A cuvette containing 1.0 µM SA and 1.0 mM Tb(EDTA) at pH 12.5 (adj. with 50% NaOH added dropwise), was prepared and stored in the dark at room temperature for 5 days.   Luminescence emission spectra were obtained after this storage period for time points of 0, 15, 17, 19, 21, 23, 25 and 27 minutes.   Spectra were integrated from 530–560 nm, and the percentage of intensity lost was calculated from an initial scan of the cuvette after 1 hour equilibration time.

Results and Discussion

Absorption spectra at pH 7.5 and pH 10.0 do not show any shift upon addition of Tb^{3+} or any Tb(ligand) complex, where ligand is EDTA, DO3A or DOTA (Figure 5.11).

This supports previous reports that pH conditions must be near or above the second pK_a value of SA (13.62) in order for the lanthanide to displace the phenolic hydrogen and provide for bidentate chelation. At pH 12.5, excitation spectra (Figure 5.12) show two populations in solution, one with a broad band at 419 nm (λ_{ex} = 296 nm) and the other with the characteristic terbium emission profile (λ_{ex} = 318 nm). The 419-nm band is assigned as the excited-state intramolecular proton transfer (ESIPT) transition. The red shift of approximately 20 nm upon complexation of deprotonated SA with the terbium binary complex is consistent with that reported for previous studies.[1]

Emission spectra indicate that the $Tb(EDTA)(SA)^{3-}$ complex exhibits the greatest luminescence intensity compared to the analogous DO2A, DO3A and DOTA complexes (Figure 5.13). This is intriguing, as we anticipated the macrocyclic ligands to perform better than the acyclic EDTA ligand. The macrocylic ligands have greater binding affinities for terbium than EDTA (Table 5.2),[35, 66, 67] and should therefore stabilize Tb^{3+} in highly basic conditions to a greater degree, reducing precipitation of the terbium hydroxide species. Secondly, in this high pH regime, the EDTA ligand should have a -4 charge (Table 5.3),[68] meaning the $Tb(EDTA)^-$ binary complex is *negatively charged*. The doubly-deprotonated SA^{2-} ligand is therefore binding to a binary complex irrespective of electrostatic attraction or repulsion. Perhaps the geometry of the open coordination sites on the lanthanide are not in the correct orientation for the hexadentate DO2A and the heptadentate DO3A. Maybe with the flexible nature of the EDTA ligand, it is more able to accomodate the sterics of the SA analyte. It has been noted by previous authors that it is impossible to explain spectroscopic behavior of Eu and Tb salicylates by position of the triplet levels alone.[69] There could be a more complex mechanism at work here.

Regardless, the Tb(EDTA)⁻ binary complex appears to be the optimal receptor site for the detection of salicylic acid.

The photodegradation study revealed that the Tb(EDTA)(SA)$^{3-}$ complex shows no loss of signal over a period of 5 days if the sample is prepared under a red lamp and kept in the dark. However, emission intensity dropped by 24% following 30 minutes of nearly constant UV exposure in the fluorescence spectrometer (7 emission scans, approximately 3 minutes of exposure per scan). We will therefore continue to prepare all samples under minimal light exposure and store them in the dark.

5.3.3   Binding Studies and Stability

With the Tb(EDTA)⁻ complex established as the optimal SA receptor site, we will explore the stability of the ternary Tb(EDTA)(SA)$^{3-}$ complex via Jobs method of continuous variations and a pH dependence study. Due to the high pH regime, the BAC assay will not be attempted due to the high proclivity of terbium hydroxide formation and precipitation.

Experimental Section

Materials.   The following chemicals were purchased and used as received: CAPS (*N*-cyclohexyl-*3*-aminopropanesulfonic acid) buffer (Alfa Aesar), CHES (*N*-cyclohexyl-*2*-aminoethanesulfonic acid) buffer (Alfa Aesar), EDTA (ethylenediamine-tetraacetic acid) (Aldrich), MOPS (*3*-(*N*-morpholino)ethanesulfonic acid) buffer (Alfa Aesar), sodium hydroxide (NaOH 50% in water) (Mallinckrodt Baker), sodium salicylate (NaSA, sodium *2*-hydroxybenzoic acid) (Fisher), TAPS (*N*-tris(hydroxymethyl) methyl-

3-aminopropanesulfonic acid) buffer (TCI America), terbium(III) chloride hexahydrate (Alfa Aesar) and Tris (tris(hydroxymethyl)aminomethane) hydrochloride buffer (J. T. Baker). The $TbCl_3$ salt, EDTA and NaSA were all 99% pure or greater, and all buffers were at least 97% pure. Water was deionized to a resistivity of 18.2 MΩ-cm using a Purelab® Ultra laboratory water purification system.

Methods. All samples were prepared in triplicate to a final volume of 4.00 mL in disposable acrylate cuvettes (Spectrocell) with a 1 cm path length. Luminescence spectral analysis was performed by a Fluorolog Fluorescence Spectrometer with a 350-nm colorless sharp cutoff glass filter as previously described (Section 5.2.2). The solution pH was measured using a calibrated handheld IQ150 pH/mV/temperature meter (I. Q. Scientific Instruments) following data collection.

Binding studies. A method of continuous variations was used to determine the binding stoichiometry for the Tb/EDTA/SA system. Samples were prepared in 50.0 mM CAPS buffer (pH 13.5) with the concentrations of Tb and SA varied inversely from 0 to 120 μM in 10 μM increments, and the concentration of EDTA maintained at 1.00 mM. Emission spectra (λ_{ex} = 314 nm) were obtained following an equilibration time of 24 hours.

pH dependence study. Solutions of 1.00 μM Tb(EDTA)(SA) were prepared in 50.0 mM buffer with 1.00 μM SA and 500 μM Tb(EDTA)$^-$ to ensure complete SA complexation. Five buffers were used: MOPS (pK_a = 7.2), TAPS (pK_a = 8.4), Tris (pK_a = 8.1), CHES (pK_a = 9.3) and CAPS (pK_a = 10.4), with pH adjustment to 0.5 increments from 7.0 to 14.0 using 50% NaOH added dropwise. Emission spectra (λ_{ex} = 314 nm) were obtained after 1 hour equilibration time.

Results and Discussion

Many attempts were made to crystallize the Tb(EDTA)(SA)$^{3-}$ ternary complex, using various counterions (TBA$^+$, Na$^+$, NH$_4$$^+$) and solvents (nanopure water, methanol, ethanol, 2-propanol, acetone, acetonitrile, ammonium hydroxide and diethyl ether). However, the only crystals obtained were of Tb(EDTA)·NaOH·2H$_2$O (Section 3.2.2). This is most likely due to either the low stability of the ternary complex or the photodegradation of the SA ligand over the crystallization period.

Binding studies indicate that the SA^{2-} ligand binds in a 1:1 ratio to the Tb(EDTA)$^-$ binary complex at high pH (13.5), confirming formation of the Tb(EDTA)(SA)$^{3-}$ ternary complex (Figure 5.14). As with the SU case (Section 5.2.3), the nonlinearity of the Jobs plot may indicate lower stability of the ternary complex. Due to the high pH regime and the high pK$_{a2}$ of salicylate, this may be due to (1) competing equilibria of the formation of Tb(OH)$_3$, and (2) the presence of a population of SA$^-$ species that is not fully deprotonated and unable to chelate Tb^{3+}. The intrinsic SA luminescence band at 419 nm can be used as an internal standard of protonated SA$^-$ concentration (Figure 5.15).

As expected, the pH dependence study reveals very little sensitized terbium luminescence until the SA ligand is fully deprotonated (Figure 5.16). Further, as the luminescence of the Tb(EDTA)(SA)$^{3-}$ increases with pH, the intrinsic SA$^-$ luminescence due to ESIPT decreases (Figure 5.17). This confirms that lanthanide chelation occurs following deprotonation of the phenol hydrogen on the SA ligand, and therefore the SA^{2-} species must be binding to the Tb(EDTA)$^-$ complex in a bidentate fashion with the carboxylate and phenolate oxygens.

5.3.4 Conclusion

Our investigation into the detection of salicylate using lanthanide binary complexes validated the results of other studies, in that the Tb(EDTA)$^-$ complex proved to have the greatest binding affinity for the SA^{2-} ligand at high pH. The fully deprotonated salicylate analyte chelates to the lanthanide ion via the phenolate and carboxylate oxygens in a bidentate manner, allowing for energy transfer to the Tb^{3+} under UV excitation at 314 nm through the AETE mechanism. It is interesting that the macrocyclic ligands did not perform nearly as well as the acyclic EDTA ligand in this case, despite their greater binding affinities for the Tb^{3+} ion and higher thermodynamic stabilities. It is possible that the rigidity of these macrocycles may impede SA binding due to steric effects, or perhaps the EDTA and SA ligands are in the proper orientation around the terbium cation to allow for intramolecular interactions that are not accessible using DO2A or DO3A. Further exploration of this system, including targeted substitutions, molecular modeling and DFT calculations, may provide insight into the unexpected binding preferences of this biologically relevant aspirin metabolite.

5.4   Catecholamines

5.4.1   Introduction

We now shift our focus to another interesting group of aromatic anions, the catecholamines (CAs). These 'fight-or-flight' hormones are part of the sympathetic nervous system, and are released by the adrenal glands in response to stress.[70] Catecholamines are produced from the amino acids phenylalanine and tyrosine, and

contain the *1,2*-dihydroxybenzene (catechol) group and either a primary or secondary amine group. Biosynthesis of catecholamines starts with the production of dopamine from L-tyrosine, which involves conversion to L-dihydroxyphenylalanine (L-DOPA) by tyrosine hydroxylase and conversion to dopamine using DOPA decarboxylase. Epinephrine and norepinephrine require further conversion steps using dopamine β-hydroxylase, a copper cofactor and phenylethanolamine *N*-methyltransferase.[71]

Catecholamines are water-soluble and circulate in the bloodstream with a half-life of approximately 3 minutes.[72] Overstimulation and/or damage of the brainstem nuclei can lead to catecholamine toxicity. This can also be caused by pheochromocytoma, neuroendocrine tumors in the adrenal medulla, and carcinoid syndrome (carcinoid tumors in the gastrointestinal tract and/or lungs). CA toxicity can also be caused by a deficiency in monoamine oxidase A, which is normally responsible for the degradation of CAs. High levels of CAs have been associated with various functional and degenerative cardiovascular disorders, such as angina pectoris, arterial hypertension and atherogenesis.[73] Decreased dopamine levels have been linked to Parkinson's disease and ADHD, while elevated levels can cause mood swing, psychosis and other neurotic disorders.[74-76] Increased levels of epinephrine (when controlled properly) can help the body reduce negative allergenic responses and regenerate lost liver cell functions.[77, 78] Thus, rapid detection of catecholamines in blood and urine can provide vital information regarding various medical conditions that might aid in more efficient diagnosis or more effective treatment.

Current methods of detection for catecholamines in biological fluids (urine, plasma and serum) involve chromatographic separation coupled to either electro-

chemical[79, 80] or fluorescence-based[81] techniques. However, most fluorescence-based methods rely purely on the native fluorescence of catecholamines (λ_{ex} ~ 280 nm, λ_{em} ~ 310 nm),[82] which has a short Stokes shift and makes it difficult to distinguish between different CAs. Others involve pre- or post-column derivatization with various fluorophores, such as naphthalene-*2,3*-dicarboxaldehyde,[83] *1,2*-diphenylethylene-diamine[84, 85] or fluorescamine.[86] These all require time for separation using expensive instrumentation, and are not feasible for CA detection in situ on the necessary time scale of 3 minutes.

Catecholamines coordinate to Cu(II), Co(II), Ni(II), Mn(II) and Zn(II) via the two phenolic hydroxyl groups.[87, 88] CAs have also been reported to complex Al^{3+} with submicromolar affinity (Table 5.4), though citrate and ATP can interfere.[5] When bound to Y^{3+}, Ca^{2+} or La^{3+}, the catecholamine still coordinates through the two phenolic groups at neutral pH, but one of the two groups remains protonated.[89-91] We therefore anticipate chelation to lanthanides at high pH where both of the phenol groups are deprotonated, allowing for bidentate coordination to the Ln^{3+} cation.

We will investigate the potential of lanthanide complexes to detect catecholamines, specifically dopamine (DA), epinephrine (Epi) and norepinephrine (NE) (Figure 5.1). The triplet energy levels of the catecholamines (23,800 to 24,000 cm^{-1})[82] lie in the appropriate range for efficient energy transfer to the $^5D_4$ energy level of Tb^{3+} (20,500 cm^{-1}).[29] Previous work using the Tb(EDTA)$^-$ complex following capillary electrophoresis has reported detection limits on the order of 0.1 μM for catecholamines (DA, NE, Epi and others).[92] However, the EDTA ligand in this case was only used to reduce terbium precipitation in basic conditions (pH 11), and not as a helper ligand with a

tailored binding site specific for the catecholamine of interest. We hope to use lanthanide(macrocycle) complexes to this aim, avoiding capillary electrophoresis or other purification/separation techniques, and attaining better limits of detection in a much shorter time period for these biologically relevant analytes.

5.4.2   Spectroscopy

Due to the high pK_as of the phenol hydrogens for catecholamines (Table 5.1),[93, 94] we will be working in very basic conditions to ensure deprotonation of these hydroxyl groups and promote lanthanide complexation. In addition to dopamine, epinephrine and norepinephrine, we will also use catechol (Cat) alone as a control species, to ensure deprotonation of the two hydroxyl species and bidentate chelation to the lanthanide.[95] We will perform a ligand screen using various Tb(ligand) complexes, where the ligand is EDTA, DO2A, DO3A or DOTA, to determine the optimal binary complex for CA chelation. The ligand should prevent precipitation of the terbium as $Tb(OH)_3$ in this high pH regime and allow effective binding of the CA analyte. We anticipate that DO3A, which binds in a heptadentate fashion and leaves space for one bidentate chelator on the Tb^{3+} ion, should be the best ligand for CA complexation.

Experimental Section

Materials.   The following chemicals were purchased and used as received: CAPS (*N*-cyclohexyl-3-aminopropanesulfonic acid) buffer (Alfa Aesar), catechol (bis-benzenediol, *1,2*-dihydroxybenzene) (TCI America), dopamine hydrochloride (*2*-(*3,4*-dihydroxyphenyl)ethylamine hydrochloride) (Alfa Aesar), DOTA (*1,4,7,10*-tetraaza-

cyclododecane-*1,4,7,10*-tetraacetate) (Macrocyclics), EDTA (ethylenediaminetetraacetic acid) (Aldrich), L-epinephrine (L-adrenaline) (Alfa Aesar), norepinephrine (L-noradrenaline) (Alfa Aesar), sodium hydroxide (NaOH 50% in water) (Mallinckrodt Baker) and terbium(III) chloride hexahydrate (Alfa Aesar). The $TbCl_3$ salt and CAPS buffer were 99.99% pure and all CAs were at least 98% pure. DO2A was prepared as previously described (Section 2.2.1). DO3A was prepared as previously described (Section 5.2.2). Water was deionized to a resistivity of 18.2 MΩ-cm using a Purelab® Ultra laboratory water purification system.

Methods. All samples were prepared to a final volume of 4.00 mL in disposable acrylate cuvettes (Spectrocell) with a 1 cm path length. Catecholamine stock solutions (4.0 mM) were kept refrigerated (4 °C) in the dark until use. Tb(ligand) stock solutions (4.0 mM, pH 7.5) were allowed to equilibrate for 1 week before use to ensure complete lanthanide complexation. Luminescence spectral analysis was performed by a Fluorolog Fluorescence Spectrometer with a 350-nm colorless sharp cutoff glass filter as previously described (Section 5.2.2). The solution pH was measured using ColorpHast™ pH indicator strips (EMD Chemicals) following data collection.

It should be noted that many catecholamines are light-sensitive, and must be prepared and stored carefully to prevent degradation. Norepinephrine is the most sensitive to light. Fresh NE solutions will have a brownish color (depending on concentration), and should be refrigerated or preferably frozen for storage. Epinephrine solutions should be clear; upon degradation, which for refrigerated samples can take a few weeks, the solution will turn pink and then brown. Dopamine is less soluble, and

makes clear solutions. As with NE, there is no visual indication when DA solutions have started to degrade, so it is recommended they are prepared fresh for each experiment.

Cuvettes of 10.0 μM CA (Cat, DA, Epi or NE) and 1.0 mM of Tb(ligand), where ligand is EDTA, DO2A, DO3A or DOTA, were prepared in 50 mM CAPS buffer, pH 13.5 (adj. with 50% NaOH added dropwise). Excitation (λ_{em} = 544 nm) and emission (λ_{ex} = 255 nm, 290 nm) spectra were obtained following 1 hour equilibration time.

Results and Discussion

Excitation spectra of the Tb(ligand)(CA) complexes (Figure 5.18) illustrate one band near 255 nm and another centered around 290–295 nm. The former is assigned as the singlet $\pi \rightarrow \pi^*$ transition L_a (in the notation of Platt[96]) of the catechol dianion (256 nm),[97] while the latter is consistent with the L_b transition of the catechol dianion, which is red-shifted from 308 nm to 290 nm when bound to a metal.[98] The Tb(DOTA)(CA) spectra all exhibit the sharp bands of the Tb^{3+} excitation spectrum, as expected considering the high concentration of terbium (1.0 mM) and the exclusion of all but one water from the lanthanide coordination sphere. For all of the catecholamines (DA, Epi and NE), the excitation intensity of the Tb(ligand)(CA) complexes was of the order DO2A > EDTA > DO3A ~ DOTA. For catechol (Cat), the order was slightly different: DO2A > DO3A ~ DOTA > EDTA. It should be noted that for all four analytes, precipitation was observed in the DO3A and DOTA cuvettes, so we will focus on the EDTA and DO2A ligands for our analysis.

Emission spectra were obtained at both λ_{max} values (255 and 290 nm) seen in the excitation spectra, but as the intensities obtained for excitation at 255 nm were about an

order of magnitude greater, we will focus on these spectra (Figure 5.19). In all cases except dopamine, the Tb(DO2A)(CA) complex had the greatest luminescence intensity. Due to the intense excitation spectrum for the Tb(DO2A)(DA)⁻ complex, we believe the extremely low intensity of the emission spectrum for this complex is in error, possibly due to the slits of the fluorescence spectrometer opening improperly. As these measurements were not performed in triplicate, these spectra should be collected again under the same conditions before conclusions can be drawn for dopamine.

For the other three analytes studied (catechol, epinephrine and norepinephrine), the emission spectral profiles for the Tb(DO2A)(CA) complexes are all very similar, as are the splittings of all four Tb(EDTA)(CA) emission spectra. Since the Stark splitting of the emission bands is indicative of the composition and geometry of the lanthanide coordination sphere, this suggests that these three ligands chelate to the Tb^{3+} cation in the same fashion for a given Tb(ligand) binary complex. The excitation spectra indicate that these are all the catechol dianion species, and therefore bidentate coordination via the deprotonated hydroxyl moieties is the most likely mode of binding. The relative intensities of the Tb(DO2A)(CA) spectra indicate that epinephrine and norepinephrine coordinate with slightly greater affinity than catechol. We attribute this to the electron-withdrawing effects of the substituents on the opposite side of the ring from the dihydroxy binding site.

It is interesting that only the binary complexes with hexadentate ligands (EDTA and DO2A) showed any significant binding for all bidentate catecholamines examined. Although this may be simply a result of poor solubility of the Tb(DO3A) complex in this pH regime, there may be steric factors involved as well. Perhaps the two remaining

coordination sites available on the Tb(DO3A) complex are not in the correct configuration to accommodate the dihydroxy catechol face of the analyte. A steric argument could also explain why the DO2A ligand is preferred over EDTA; though both have three adjacent binding sites available for CA chelation, they are arranged in a linear pattern for Tb(DO2A)$^+$ and in a triangular pattern for Tb(EDTA)$^-$. This preliminary analysis implies that further experimentation is necessary to understand the complex relationship between ligand denticity, binding site geometry and catecholamine binding affinity.

5.4.3   Conclusion

Though we have only begun to explore the potential of lanthanide(macrocycle) complexes in the detection of catecholamines, we have established through simple spectroscopic analysis that DO2A is superior to the previously proposed EDTA in forming a luminescent Tb(ligand)(CA) complex at high pH. Future work such as evaluation of catecholamine binding affinities and lifetime measurements to determine the hydration numbers of the Tb(ligand)(CA) complexes would help significantly in our understanding of this system. Luminescence intensities would be further improved by degassing these samples and working under inert atmosphere to avoid oxidation of the catecholamines and related compounds.

5.5   Concluding Remarks

We have demonstrated the versatility of Tb(ligand) binary complexes in the detection of various salicylates and catecholamines using sensitized lanthanide luminescence. Both cyclic (DO2A) and linear (EDTA) chelators can be utilized to generate a receptor site with increased stability and greater affinity for the analyte of interest. In each case, finding the optimal match between lanthanide complex and target analyte is not always intuitive; indeed, all bidentate analytes explored here were most compatible with hexadentate ligands, which leave not two but three sites available on the nine-coordinate lanthanide ion (Table 5.5). The mechanisms that govern optimization of effective ligand-analyte pairings remain to be elucidated, though binding site geometry, interligand interactions and electron density perturbations on the central lanthanide are likely contributing factors.

The use of a helper ligand for analyte detection affords several advantages over lanthanide ions alone. The ligand stabilizes the complex over a wider pH range, allowing for detection even in very basic conditions, which is often required for analytes that must be fully deprotonated to bind effectively (i.e., SA and CAs). The chelating ligand also prevents the coordination of multiple analyte molecules to the same lanthanide, and therefore establishes a linear correlation between luminescence intensity and analyte concentration. In addition, use of these ligands provides greater options for sensor specificity and design, in that modifications can be incorporated for enhanced interligand interactions or tethering the complex to a solid substrate.

We anticipate further development of lanthanide binary complexes as receptor sites for aromatic anions, with the ultimate goal of generating highly specific sensors

capable of sensitive detection in matrices such as environmental samples or biological fluids. The possibility of using several lanthanide-based receptor sites simultaneously then becomes possible. For instance, as salicylic acid is broken down into salicylurate in the liver, the ratio of SA to SU could be an efficient method to monitor liver health and function. A dual assay could be envisioned using $Tb(DO2A)^+$ at pH 8.4 to detect SU and $Tb(EDTA)^-$ at pH 13.5 to detect SA in aliquots taken from the same plasma or urine sample. Though we are only in the initial stages of meeting such goals, the work presented here represents the first step in the application of tailored lanthanide-based receptor sites in the detection of aromatic analytes.

Through the investigations reported in this dissertation, we have learned some important lessons regarding sensor design that have applications in a multitude of fields. We have discovered that the property of 'ligand enhanced' binding affinity is not unique to the dipicolinate system, and that ligand chelation can significantly improve the lanthanide-based detection of a variety of oxyanions. We have also learned that net electrostatic interaction is not the dominant factor governing coordination to lanthanide binary complexes, and in fact variations in the local charge density may be much more important. Even neutral lanthanide complexes can attract anionic ligands better than the corresponding tripositive Ln^{3+} ion alone, with improvements in binding affinity by an order of magnitude or more. This ligand enhancement is most likely due to perturbations in the electron density of the lanthanide by the electron-withdrawing moieties of the ligand, generating a more electropositive binding site for the complex than the aquo ion alone is capable. This theory could be verified by modifying a ligand like DO2A to contain strongly electronegative species (such as fluorine) on the opposite side as the

dipicolinate binding site. If indeed the lanthanide electron density is affected, this should result in an even more positive binding site, and hence a greater dipicolinate binding affinity. Further experiments with photoelectron or Raman spectroscopy are expected to ascertain the degree of perturbation of the lanthanide by the helper ligand.

Our work also indicates that ligand interactions with lanthanide complexes cannot be predicted based on the number of available binding sites or their geometry. Bidentate ligands sometimes prefer a lanthanide complex with three remaining coordination sites instead of two, and monodentate ligands in some cases can bind more strongly to a lanthanide ion encapsulated by a heptadentate ligand as opposed to an octadentate one. We have also found that both cyclic and acyclic ligands can produce lanthanide complexes that are effective receptor sites for analytes. We therefore recommend that, to determine the optimal partnering between lanthanide complex and analyte, ligand screens should always be performed to enhance receptor site performance and specificity. This could be best accomplished with binding studies to quantify analyte binding affinity, such as the binding affinity by competition (BAC) assay proposed here.

The advantages of ligand enhancement can be implemented in current detection schemes where lanthanide ions alone are used to chelate other molecules of interest. As mentioned in Chapter 1, there are various areas of research involving sensitized lanthanide luminescence, ranging from PCR and gene detection techniques which monitor disease and toxins, to drug discovery applications and high-throughput screening assays. The application of lanthanide(ligand) complexes instead of lanthanide ions alone could significantly enhance the efficacy of these methods. For instance, detection of tyrosine kinase activity by terbium luminescence could be improved markedly with the

addition of a chelating ligand such as DO2A or DO3A. The terbium cation binds to phosphorylated tyrosine, which is used to mitigate diseases involving tyrosine kinase-mediated signaling.[99] With the binding enhancement of a chelating ligand, the limit of detection of phosphorylated tyrosine is expected to be improved by an order of magnitude or more. One can envision taking further advantage of this effect by addition of electronegative groups such as fluorine to the helper ligand to generate an even more electropositive binding cavity. Such binary complexes could also find use in time-resolved Förster resonance energy transfer (FRET) systems, where improved lanthanide luminescence lifetime as a result of ligand coordination could manifest in enhanced limits of detection.

Further, evidence of a ligand-induced 'gadolinium break' effect can have implications in various studies involving lanthanide chelation. One cannot assume that a given trend in a physical or chemical property for the lanthanide series will remain constant in the presence of a chelating ligand, especially one containing nitrogen and oxygen donor atoms. In the work described here, the unique susceptibility of Tb^{3+} to electron density perturbation by a chelating ligand worked to our advantage, producing a more electropositive binding site in the $Tb(DO2A)^+$ complex than any other lanthanide complex. However, this gadolinium break effect is only one of many phenomena governing the stability and photophysics of lanthanide complexes. Those exploring lanthanide complexes for targeted detection should keep in mind that choice of lanthanide can significantly influence binding affinity and related properties, especially near gadolinium in the lanthanide series (i.e., terbium and europium).

Lanthanide chemistry is a rich and often enigmatic field; in many ways we are still only scratching the surface of applications and possibilities. We hope that the lessons learned in the course of this dissertation will promote the development of more sensitive and selective receptor sites in the sensor design pursuits of the future.

REFERENCES

(1)   Arnaud, N.; Georges, J. *Analyst* **1999**, *124*, 1075-1078.

(2)   Bailey, M. P.; Rocks, B. F.; Riley, C. *Analytica Chimica Acta* **1987**, *201*, 335-338.

(3)   Lianidou, E. S.; Ioannou, P. C.; Polydorou, C. K.; Efstathiou, C. E. *Analytica Chimica Acta* **1996**, *320*, 107-114.

(4)   Tuckerman, M. M.; Mayer, J. R.; Nachod, F. C. *Journal Of The American Chemical Society* **1959**, *81*, 92-94.

(5)   Kiss, T.; Sóvágó, I.; Martin, R. B. *Journal Of The American Chemical Society* **1989**, *111*, 3611-3614.

(6)   Services, D. o. H. a. H., Ed.; Food and Drug Administration, 1998; Vol. 63, pp 56802-56819.

(7)   Bayer, A. *Clinicians' Guide to Aspirin*; Chapman & Hall Medical: London, 1998.

(8)   Taylor, D. W.; Barnett, H. J. M.; Haynes, R. B.; Ferguson, G. G.; Sackett, D. L.; Thorpe, K. E.; Simard, D.; Silver, F. L.; Hachinski, V.; Clagett, G. P.; Bames, R.; Spence, J. D. *The Lancet* **1999**, *353*, 2179-2184.

(9)   Group, T. C. C. S. *New England Journal of Medicine* **1978**, *299*, 53-59.

(10)   Coolen, S. A. J.; Huf, F. A.; Reijenga, J. C. *Journal of Chromatography B* **1998**, *717*, 119-124.

(11)   Williams, F. M. *Clinical Pharmacokinetics* **1985**, *10*, 392-403.

(12)   Liu, J.-H.; Smith, P. C. *Journal of Chromatography B* **1996**, *675*, 61-70.

(13)   Miners, J. O. *Clinical Pharmacokinetics* **1989**, *17*, 327-344.

(14)   Levy, G.; Amsel, L. P.; Elliott, H. C. *Journal of Pharmaceutical Sciences* **1969**, *58*, 827-829.

(15)   Levy, G. *Journal of Pharmaceutical Sciences* **1965**, *54*, 959-967.

(16)   Paterson, J. R.; Baxter, G. J.; Dreyer, J. S.; Halket, J. M.; Flynn, R.; Lawrence, J. R. *Journal of Agricultural and Food Chemistry* **2008**, *56*, 11648-11652.

(17)   Bar-Or, D.; Office, U. S. P. a. T., Ed.; Appenditech, Inc.: United States, 1995, pp 1-16.

(18)   Buskin, J. N.; Upton, R. A.; Williams, R. L. *Clinical Chemistry* **1982**, *28*, 1200-1203.

(19)   Peng, G. W.; Gadalla, M. A. F.; Smith, V.; Peng, A.; Chiou, W. L. *Journal of Pharmaceutical Sciences* **1977**, *67*, 710-712.

(20)   Cham, B. E.; Bochner, F.; Imhoff, D. M.; Johns, D.; Rowland, M. *Clinical Chemistry* **1980**, *26*, 111-114.

(21)   Zaugg, S.; Zhang, X.; Sweedler, J.; Thormann, W. *Journal of Chromatography B* **2001**, *752*, 17-31.

(22)   Salinas, F.; Berzas Nevado, J. J.; Espinosa Mansilla, A. *Talanta* **1990**, *37*, 347-351.

(23)   Bavoso, A.; Menabue, L.; Saladini, M.; Sola, M. *Inorganic Chemica Acta* **1996**, *244*, 207-212.

(24)   Ferrer, E. G.; Gonzalez Baro, A. C.; Castellano, E. E.; Piro, O. E.; Williams, P. A. M. *Journal of Inorganic Biochemistry* **2004**, *98*, 413-421.

(25)   Kiss, T.; Jakusch, T.; Kilyen, M.; Kiss, E.; Lakatos, A. *Polyhedron* **2000**, *19*, 2389-2401.

(26)   Jancso, A.; Gajda, T.; Szorcsik, A.; Kiss, T.; Henry, B.; Vanko, G.; Rubini, P. *Journal of Inorganic Biochemistry* **2001**, *83*, 187-192.

(27)   Parker, D. *Chemical Communications* **2005**, 3141-3143.

(28)   Pal, R.; Parker, D.; Costello, L. C. *Organic and Biomolecular Chemistry* **2009**, *7*, 1525-1528.

(29)   Carnall, W. T.; Fields, P. R.; Rajnak, K. *Journal Of Chemical Physics* **1968**, *49*, 4447-4449.

(30)   Wang, Q.-M. *Journal of Organometallic Chemistry* **2006**, *691*, 545-550.

(31)   Arnaud, N.; Vaquer, E.; Georges, J. *Analyst* **1998**, *123*, 261-265.

(32)   Carnall, W. T.; Fields, P. R.; Rajnak, K. *Journal Of Chemical Physics* **1968**, *49*, 4424-4442.

(33)   Carnall, W. T.; Fields, P. R.; Rajnak, K. *Journal Of Chemical Physics* **1968**, *49*, 4450-4455.

(34)   Hemmila, I.; Laitala, V. *Journal Of Fluorescence* **2005**, *15*, 529-542.

(35)   Kim, W. D.; Hrncir, D. C.; Kiefer, G. E.; Sherry, A. D. *Inorganic Chemistry* **1995**, *34*, 2225-2232.

(36)   Mishra, A., 2008.

(37)   Maheshwari, S.; Chowdhury, A.; Sathyamurthy, N. *Journal of Physical Chemistry A* **1999**, *103*, 6257-6262.

(38)   Lahmani, F.; Zehnacker-Rentien, A. *Journal of Physical Chemistry A* **1997**, *101*, 6141-6147.

(39)   Ainsworth, C. C.; Friedrich, D. M.; Gassman, P. L.; Wang, Z.; Joly, A. G. *Geochimica et Cosmochimica Acta* **1998**, *62*, 595-612.

(40)   Weller, A. *Progress in Reaction Kinetics and Mechanisms* **1961**, *1*, 188-214.

(41)   Heimbrook, L.; Kenny, J. E.; Kohler, B. E.; Scott, G. W. *Journal of Physical Chemistry* **1983**, *87*, 280-289.

(42)   Barbara, P. F.; Walsh, P. K.; Brus, L. E. *Journal of Physical Chemistry* **1989**, *93*, 29-34.

(43)   Horrocks Jr., W. D.; Sudnick, D. R. *Journal Of The American Chemical Society* **1979**, *101*, 334-340.

(44)   Beeby, A.; Clarkson, I. M.; Dickins, R. S.; Faulkner, S.; Parker, D.; Royle, L.; de Sousa, A. S.; Williams, J. A. G.; Woods, M. *Journal of the Chemical Society-Perkin Transactions 2* **1999**, 493-503.

(45)   Cable, M. L.; Kirby, J. P.; Levine, D. J.; Manary, M. J.; Gray, H. B.; Ponce, A. *Journal Of The American Chemical Society* **2009**, *131*, 9562-9570.

(46)   Bosund, L. *Advances in Food Research* **1962**, *11*, 331-353.

(47)   Gollnick, H.; Schramm, M. *Dermatology* **1998**, *196*, 119-125.

(48)   Russell, A. D. In *Principles and Practice of Disinfection, Preservation and Sterilization,* Third ed.; Russell, A. D., Hugo, W. B., Ayliffe, G. A. J., Eds.; Blackwell Science Ltd.: Oxford, 1999, pp 95-123.

(49)   Davies, M. G.; Briffa, D. V.; Greaves, M. W. *British Journal of Medicine* **1979**, *1*, 661.

(50)   Bernstein, J. M.; Weiss, A. D. *Journal of Laryngology & Otology* **1967**, *81*, 915-926.

(51)   Chaniotakis, N. A.; Park, S. B.; Meyerhoff, M. E. *Analytical Chemistry* **1989**, *61*, 566-570.

(52)   Goto, Y.; Makino, K.; Kataoka, Y.; Shuto, H. *Journal of Chromatography B* **1998**, *706*, 329-335.

(53)   Brodie, B. B.; Udenfriend, S.; Coburn, A. F. *Journal of Pharmacology And Experimental Therapeutics* **1944**, *80*, 114-117.

(54)   Lange, W. E.; Bell, S. A. *Journal of Pharmaceutical Sciences* **1966**, *55*, 386-389.

(55)   Saltzman, A. *Journal of Biological Chemistry* **1948**, *174*, 399-404.

(56)   Bae, S. K.; Seo, K. A.; Jung, E. J.; Kim, H.-S.; Yeo, C.-W.; Shon, J.-H.; Park, K.-M.; Liu, K.-H.; Shin, J.-G. *Biomedical Chromatography* **2008**, *22*, 590-595.

(57)   Kees, F.; Jehnich, D.; Grobecker, H. *Journal of Chromatography B* **1996**, *677*, 172-177.

(58)   Cham, B. E.; Johns, D.; Bochner, F.; Imhoff, D. M.; Rowland, M. *Clinical Chemistry* **1979**, *25*, 1420-1425.

(59)   Torriero, A. A. J.; Luco, J. M.; Sereno, L.; Raba, J. *Talanta* **2004**, *62*, 247-254.

(60)   Trinder, P. *Biochemical Journal* **1954**, *57*, 301-303.

(61)   Silva, T. R.; Valdman, E.; Valdman, B.; Leite, S. G. F. *Brazilian Journal of Microbiology* **2007**, *38*, 39-44.

(62)   Perrin, D. D. *Nature* **1958**, *182*, 741-742.

(63)   Li, C.; Wong, W.-T. *Tetrahedron Letters* **2004**, *45*, 6055-6058.

(64)   Minnick, L. J.; Kilpatrick, M. *Journal Of Physical Chemistry* **1939**, *43*, 259-274.

(65)   Porto, R.; De Tommaso, G.; Furia, E. *Annali di Chimica* **2005**, *95*, 551-558.

(66)   Martell, A. E.; Smith, R. M. *Critical Stability Constants*; Plenum Press: New York, 1974.

(67)   Chang, C. A.; Chen, Y.-H.; Chen, H.-Y.; Shieh, F.-K. *Journal Of The Chemical Society-Dalton Transactions* **1998**, 3243-3248.

(68)   Schwarzenbach, G.; Freitag, E. *Helvetica Chimica Acta* **1951**, *34*, 1503-1508.

(69)   Tsaryuk, V. I.; Zhuravlev, K.; Zolin, V. F.; Gawryszewska, P.; Legendziewicz, J.; Kudryashova, V. A.; Pekareva, I. *journal Of Photochemistry And Photobiology A-Chemistry* **2006**, *177*, 314-323.

(70)   Hockenbury, D. H.; Hockenbury, S. E. *Psychology*, Fourth Edition ed.; Worth Publishers: New York, 2006.

(71)   Goldstein, D. S.; Eisenhofer, G.; McCarty, R. *Catecholamines: Bridging Basic Science with Clinical Medicine*; Academic Press: San Diego, 1998.

(72)   Whitby, L.; Axelrod, J.; Weil-Malherbe, H. *Journal of Pharmacology And Experimental Therapeutics* **1961**, *132*, 191-201.

(73)   Raab, W. *The American Journal of Cardiology* **1960**, *5*, 571-578.

(74)   Madras, B. K.; Miller, G. M.; Fischman, A. J. *Behavioural Brain Research* **2002**, *130*, 57-63.

(75)   Greer, M.; Williams, C. M. *Neurology* **1963**, *13*, 73-76.

(76)   Barbeau, A. *Canadian Medical Association Journal* **1962**, *87*, 802-807.

(77)   Middleton, E.; Finke, S. R. *Journal of Allergy* **1968**, *42*, 288-299.

(78)   Lockey, S. D.; Glennon, J. A.; Reed, C. E. *Journal of Allergy* **1967**, *40*, 349-354.

(79)   Riggin, R. M.; Kissinger, P. T. *Analytical Chemistry* **1977**, *49*, 2109-2111.

(80)   Hallman, H.; Farnebo, L.-O.; Hamberger, B.; Jonsson, G. *Life Sciences* **1978**, *23*, 1049-1052.

(81)   van der Hoorn, F. A. J.; Boomsma, F.; Man In't Veld, A. J.; Schalekamp, M. A. D. H. *Journal of Chromatography B: Biomedical Sciences and Applications* **1989**, *487*, 17-28.

(82)   Yamaguchi, M.; Yutani, Y.; Kohashi, K.; Ohkura, Y. *Analytica Chimica Acta* **1979**, *108*, 297-308.

(83)   Robert, F.; Bert, L.; Denoroy, L.; Renaud, B. *Analytical Chemistry* **1995**, *67*, 1838-1844.

(84)   Nohta, H.; Mitsui, A.; Ohkura, Y. *Analytica Chimica Acta* **1984**, *165*, 171-176.

(85)   Nohta, H.; Mitsui, A.; Umegae, Y.; Ohkura, Y. *Biomedical Chromatography* **1986**, *2*, 9-12.

(86)   Imai, K.; Tsukamoto, M.; Tamura, Z. *Journal of Chromatography A* **1977**, *137*, 357-362.

(87)   Jameson, R. F.; Neillie, W. F. S. *Journal of Inorganic and Nuclear Chemistry* **1965**, *27*, 2623-2634.

(88)   Jameson, R. F.; Neillie, W. F. S. *Journal of Inorganic and Nuclear Chemistry* **1966**, *28*, 2667-2675.

(89)   Aydin, R. *Journal of Chemical and Engineering Data* **2007**, *52*, 2400-2404.

(90)   Wu, Z. J.; Gao, F.; Wang, J. P.; Niu, C. J.; Niu, V. J. *Journal Of Coordination Chemistry* **2005**, *58*, 473-478.

(91)   Chakrawarti, P. B.; Vijayvargiya, B. L.; Sharma, H. N. *Journal of the Indian Chemical Society* **1983**, *60*, 89-91.

(92)   Zhu, R. H.; Kok, W. T. *Analytical Chemistry* **1997**, *69*, 4010-4016.

(93)   Kiss, T.; Gergely, A. *Inorganica Chimica Acta* **1979**, *36*, 31-36.

(94)   Gergely, A.; Kiss, T.; Deák, G.; Sóvágó, I. *Inorganica Chimica Acta* **1981**, *56*, 35-40.

(95)   Borraccino, R.; Kharoune, M.; Giot, R.; Agathos, S. N.; Nyns, E.-J.; Naveau, H. P.; Pauss, A. *Water Research* **2001**, *35*, 3729-3737.

(96)   Platt, J. R. *Journal Of Chemical Physics* **1949**, *17*, 484-495.

(97)   Vaillancourt, F. H.; Barbosa, C. J.; Spiro, T. G.; Bolin, J. T.; Blades, M. W.; Turner, R. F. B.; Eltis, L. D. *Journal Of The American Chemical Society* **2002**, *124*, 2485-2496.

(98)   Horsman, G. P.; Jirasek, A.; Vaillancourt, F. H.; Barbosa, C. J.; Jarzecki, A. A.; Xu, C.; Mekmouche, Y.; Spiro, T. G.; Lipscomb, J. D.; Blades, M. W.; Turner, R. F. B.; Eltis, L. D. *Journal Of The American Chemical Society* **2005**, *127*, 16882-16891.

(99)   Zondlo, S. C.; Gao, F.; Zondlo, N. J. *Journal Of The American Chemical Society* **2010**, *ASAP*.

FIGURES

Salicyluric acid (SU)

Salicylic acid (SA)

Dopamine (DA)

Norepinephrine (NE)

Epinephrine (Epi)
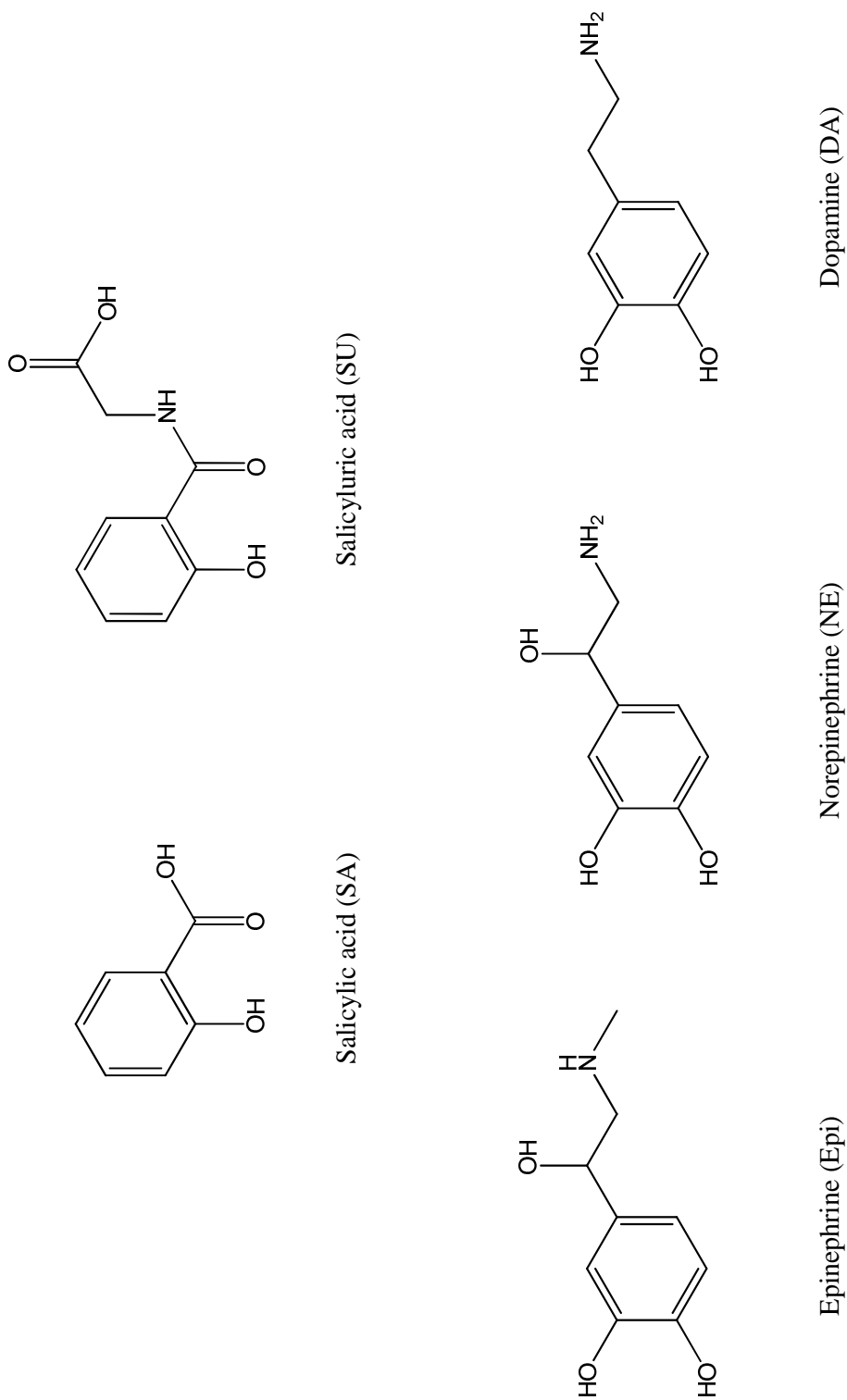
Figure 5.1. Various aromatic analytes to be investigated in terms of detection using a tailored terbium-macrocycle binary complex. Top row: salicylates. Bottom row: catecholamines.
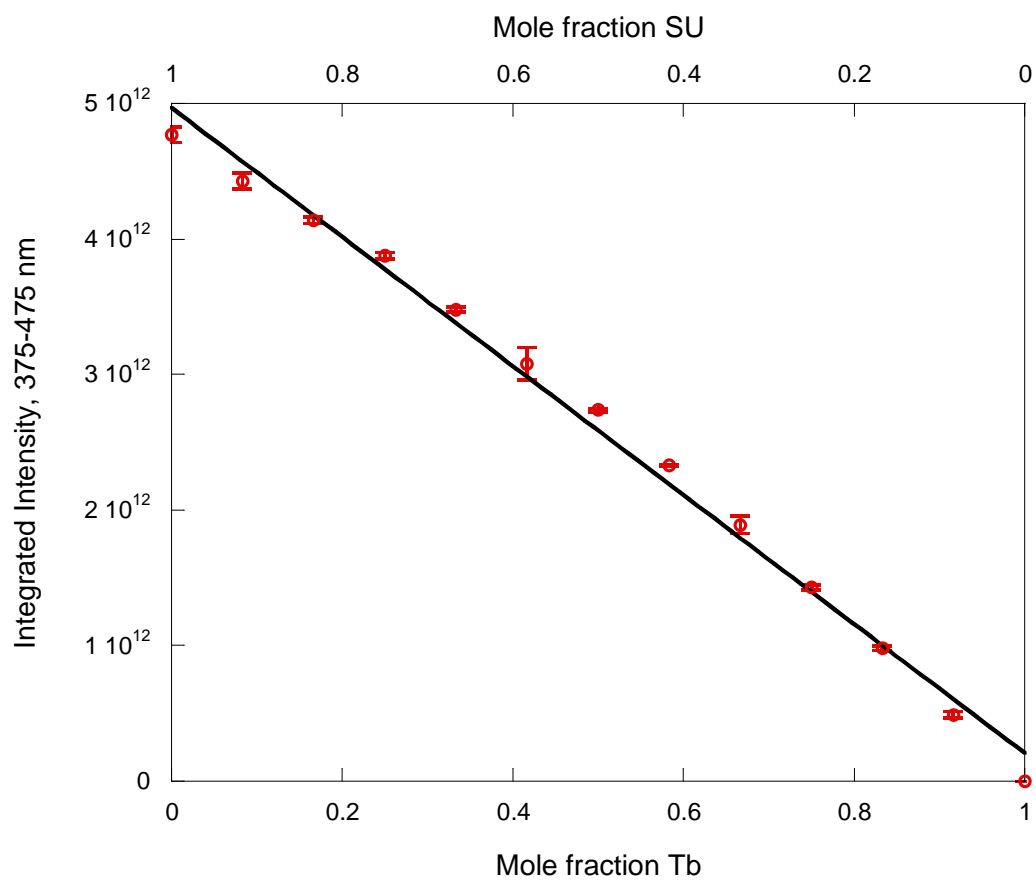
Figure 5.2. Method of continuous variations, showing linear correlation of intrinsic salicylurate (SU) luminescence (419 nm) that can be used as an internal standard. Concentrations of Tb and SU were varied inversely from 0 to 120 μM in 10 μM increments, with 500 μM DO2A in 0.1 M TAPS buffer, pH 8.4.
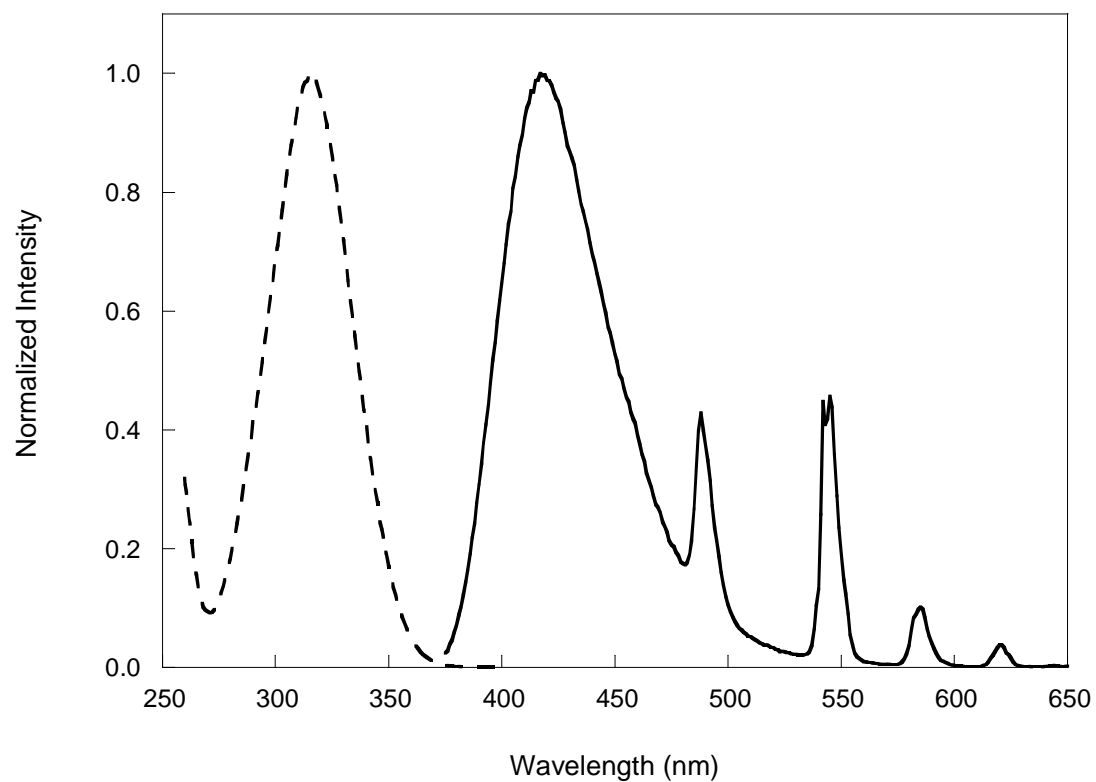
Figure 5.3. Excitation (dashed) and emission (solid) spectra of Tb(DO2A)(SU)⁻ complex, 100 µM in 0.1 M TAPS buffer, pH 8.4 (λ_{ex} = 316 nm, λ_{em} = 544 nm).
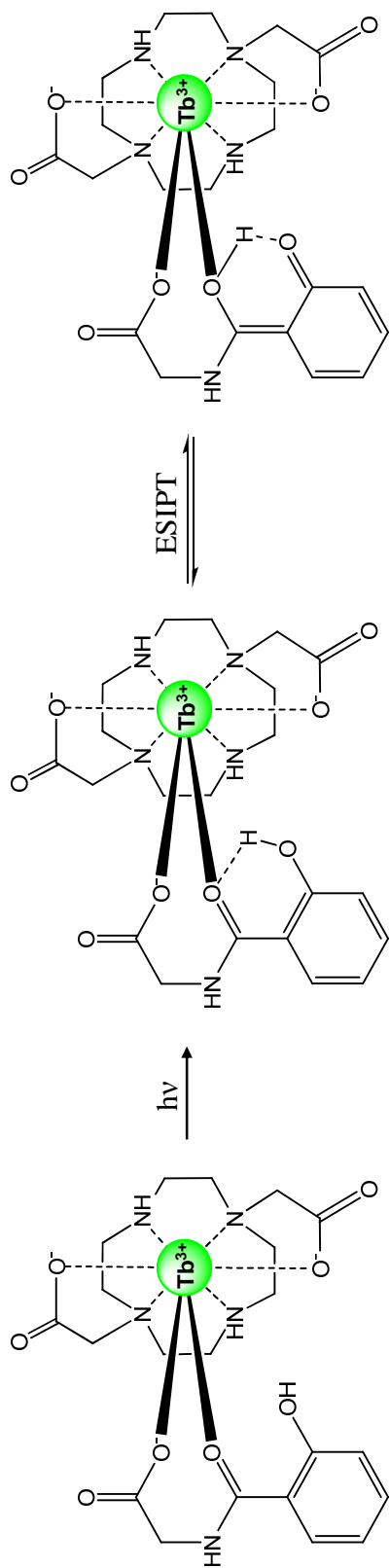
Figure 5.4. Most likely chelation mode of the salicylurate (SU) ligand to the Tb(DO2A)$^+$ complex. As shown, excited-state intramolecular proton transfer (ESIPT) can still occur on the SU ligand with this binding motif.
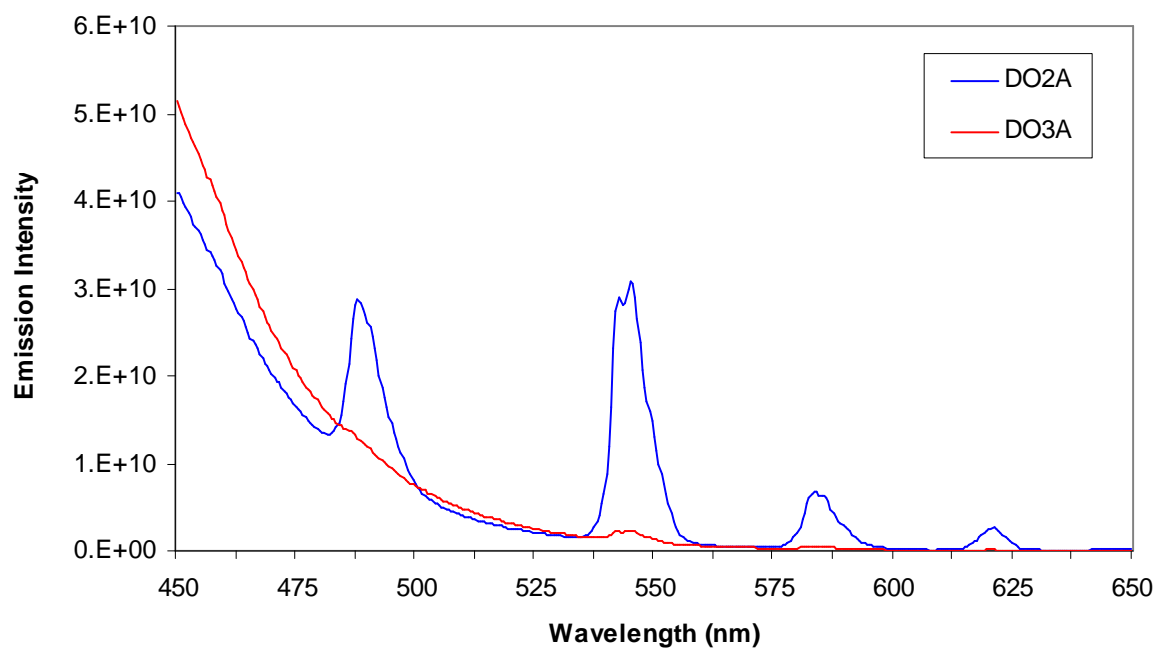
Figure 5.5. Emission spectra of Tb(DO2A)(SU)$^-$ and Tb(DO3A)(SU)$^{2-}$, 100 µM in 0.1 M TAPS, pH 8.4 (λ_{ex} = 316 nm).
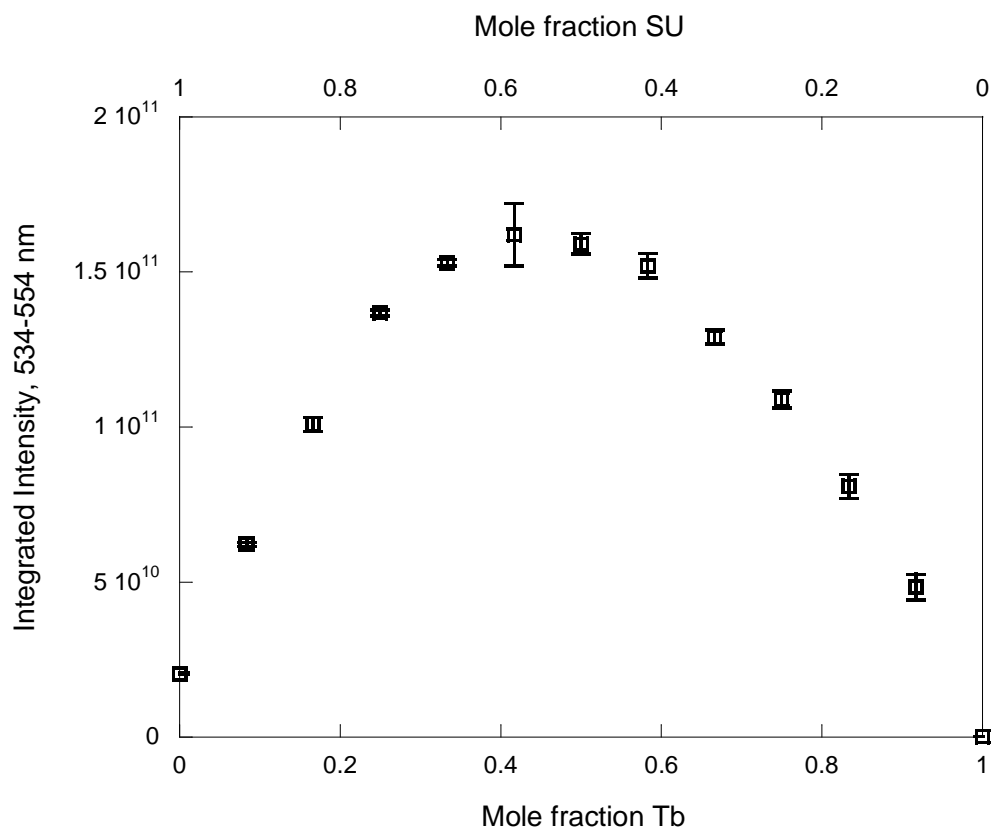
Figure 5.6. Method of continuous variations to determine binding stoichiometry of SU to Tb(DO2A)$^+$. [Tb] and [SU] varied inversely from 0–120 µM in 10 µM increments with 500 µM DO2A in 0.1 M TAPS buffer, pH 8.4 (λ_{ex} = 316 nm).
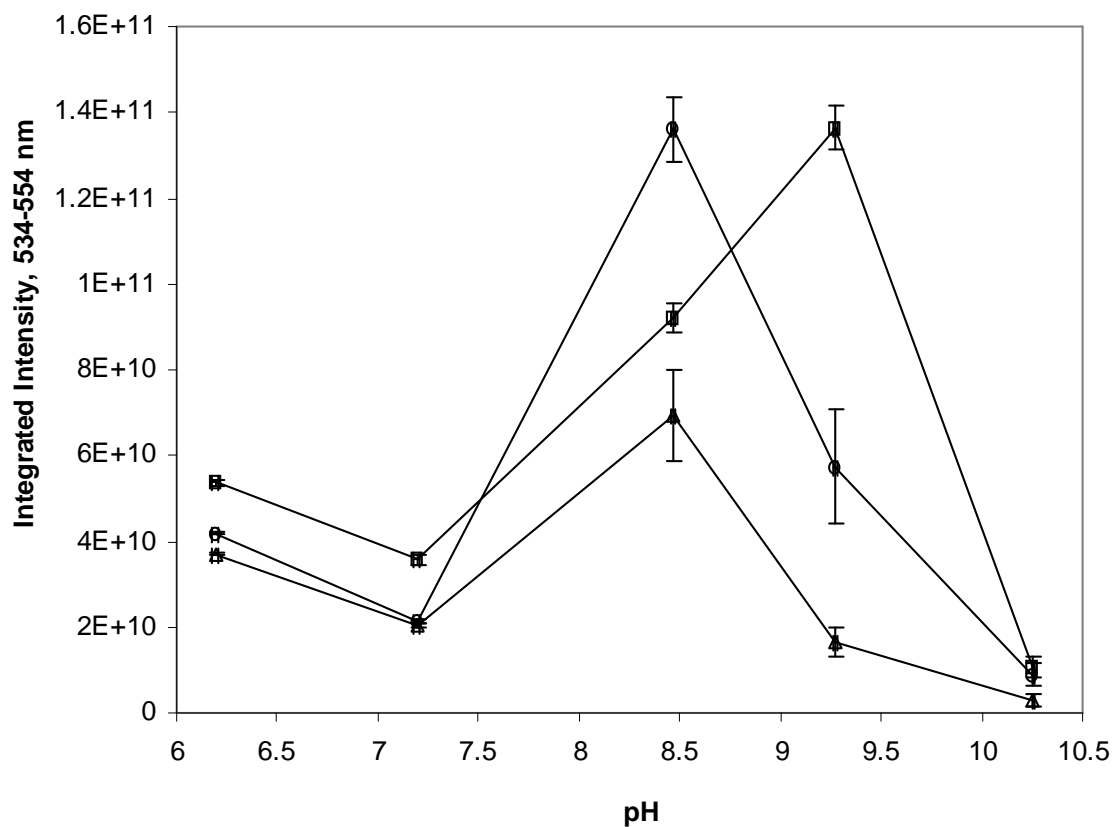
Figure 5.7. pH dependence study of Tb(DO2A)(SU)⁻ complex, 100 µM with 5X excess DO2A. Emission spectra (λ_{ex} = 316 nm) obtained following 15 min (□), 18 hr (○) or 5 days (Δ) equilibration time.
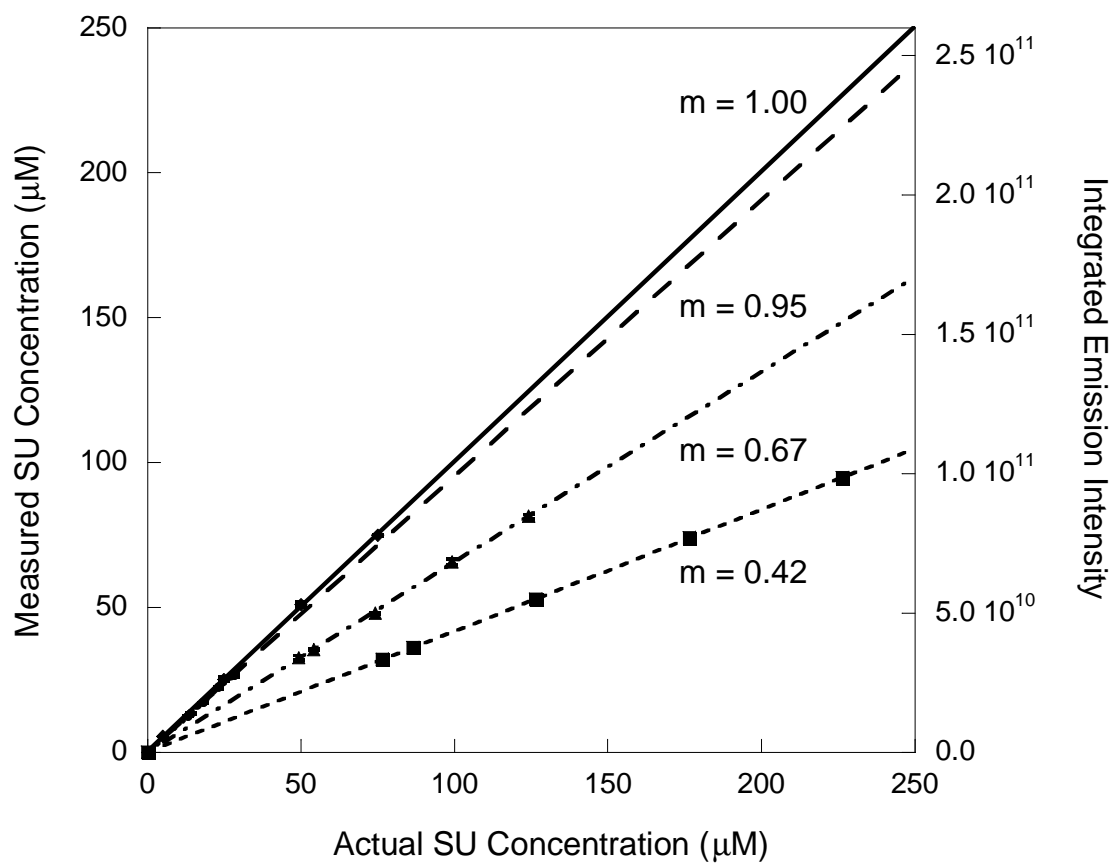
Figure 5.8. Dilution study of an SU-spiked urine sample for dilution factors of 1:3.5 (dotted), 1:7 (dashed-dotted), and 1:35 (dashed) into 5 mM Tb(DO2A)$^+$ in 0.1 M TAPS buffer, pH 8.4 (λ_{ex} = 316 nm). As the dilution factor is increased, the slope (m) approaches unity, equivalent to an aqueous solution spiked with SU (solid).
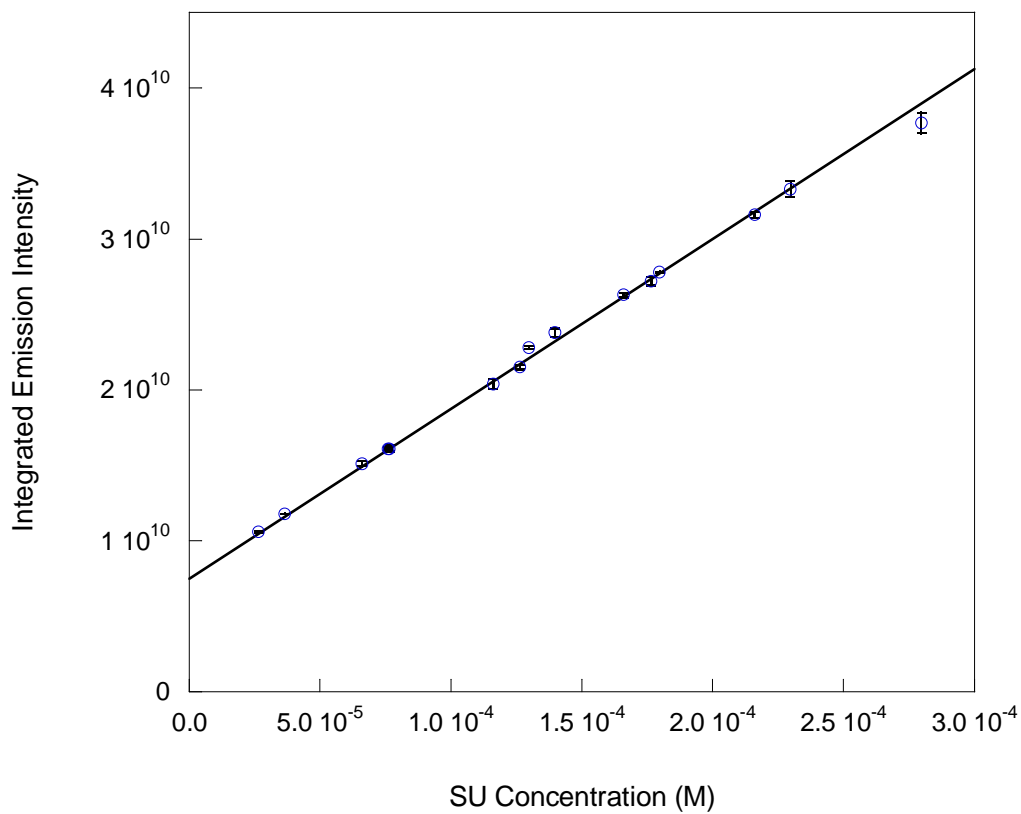
Figure 5.9. Calibration curve of SU spiked into urine samples (dilution factor 1:350) from three individual healthy donors, relating luminescence intensity to SU concentration. Samples diluted into 5 mM Tb(DO2A)$^+$ in 0.1 M TAPS buffer, pH 8.4 (λ_{ex} = 316 nm).
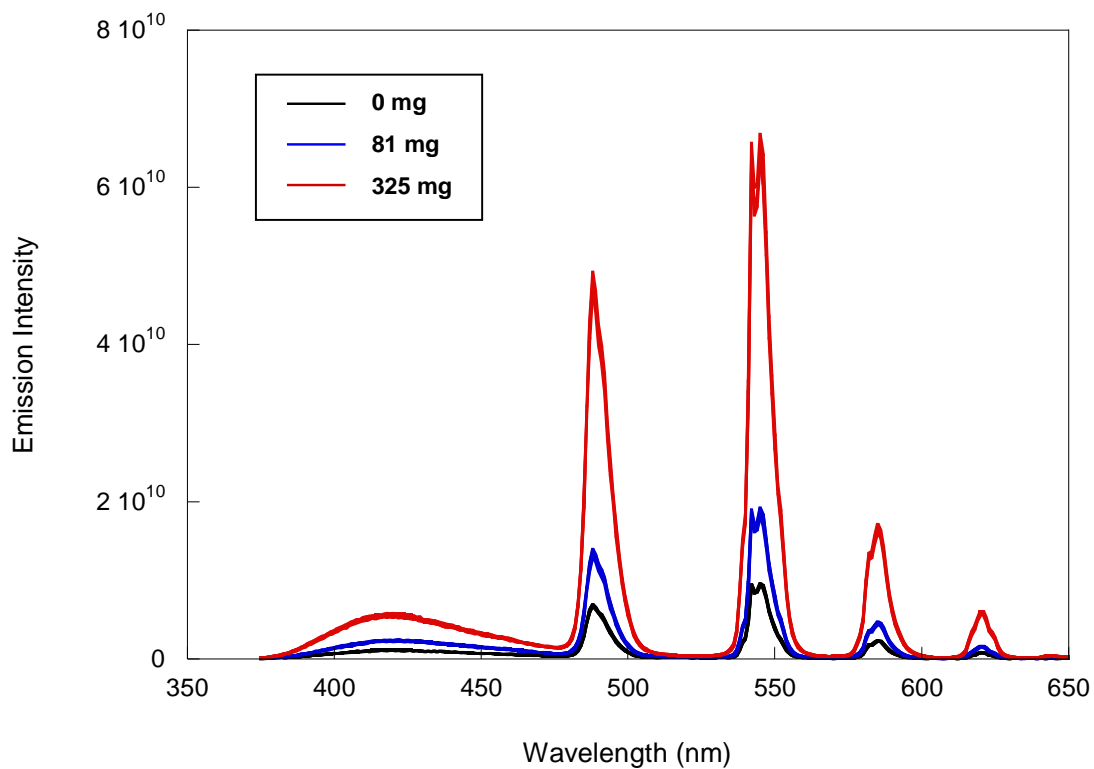
Figure 5.10. Aspirin study showing an increase in luminescence due to increased ASA dosage. Samples diluted 1:350 into 5 mM Tb(DO2A)$^+$ in 0.1 M TAPS buffer, pH 8.4 (λ_{ex} = 316 nm). Emission spectra, taken for three separate samples, are nearly superimposable for each aspirin dosage.
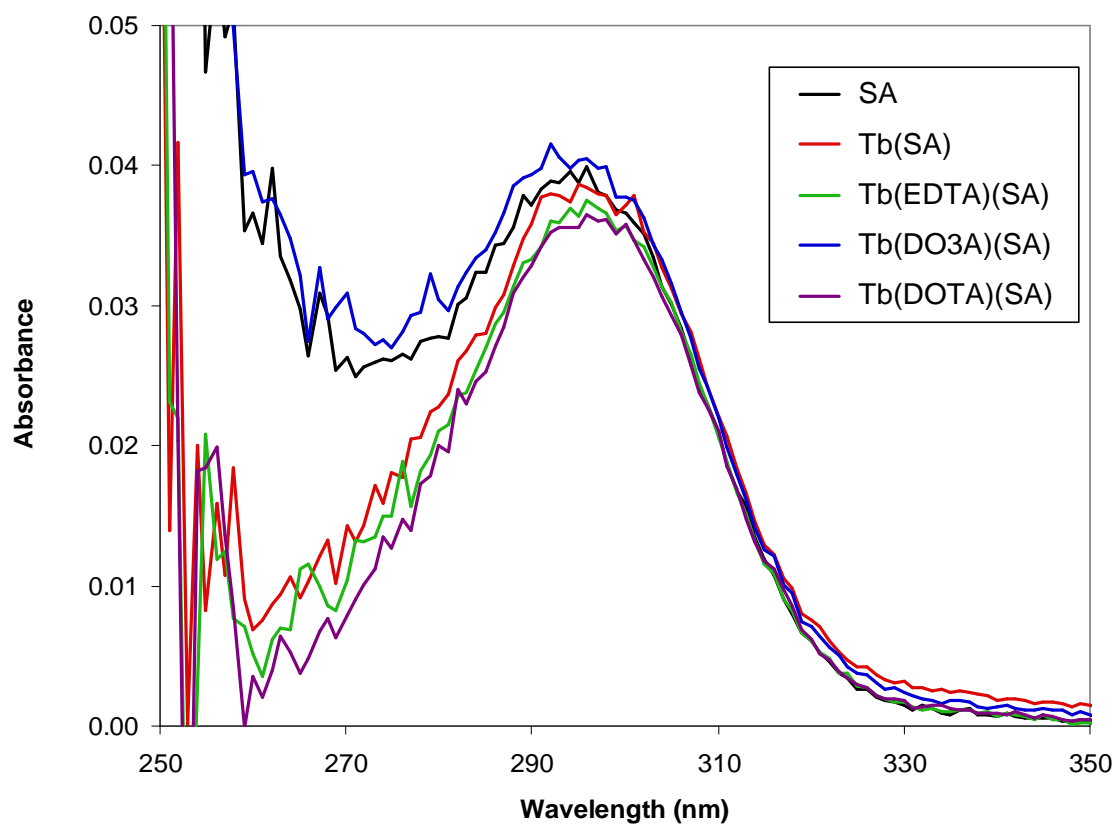
Figure 5.11. Absorption spectra for 10.0 µM SA, Tb(SA), Tb(EDTA(SA), Tb(DO3A)(SA) and Tb(DOTA)(SA) in 0.1 M CAPS (pH 10.0).
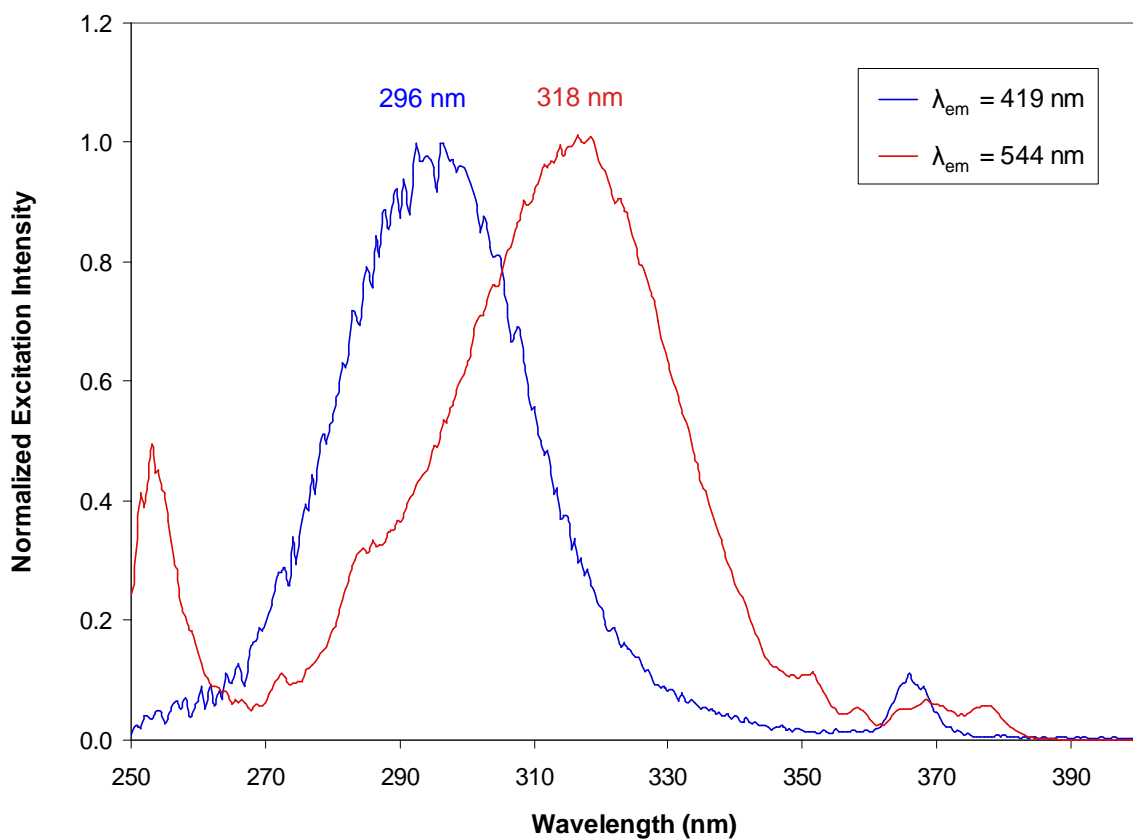
Figure 5.12. Normalized excitation spectra of Tb(EDTA)(SA) complex in 50 mM CAPS buffer (pH 12.5) at two emission wavelengths. The two populations are unchelated SA (blue) and the Tb(EDTA)(SA) complex (red) according to the emission spectra at 296 nm and 318 nm, respectively, which show ESIPT from SA alone or the characteristic terbium emission bands from the Tb(EDTA)(SA) complex.
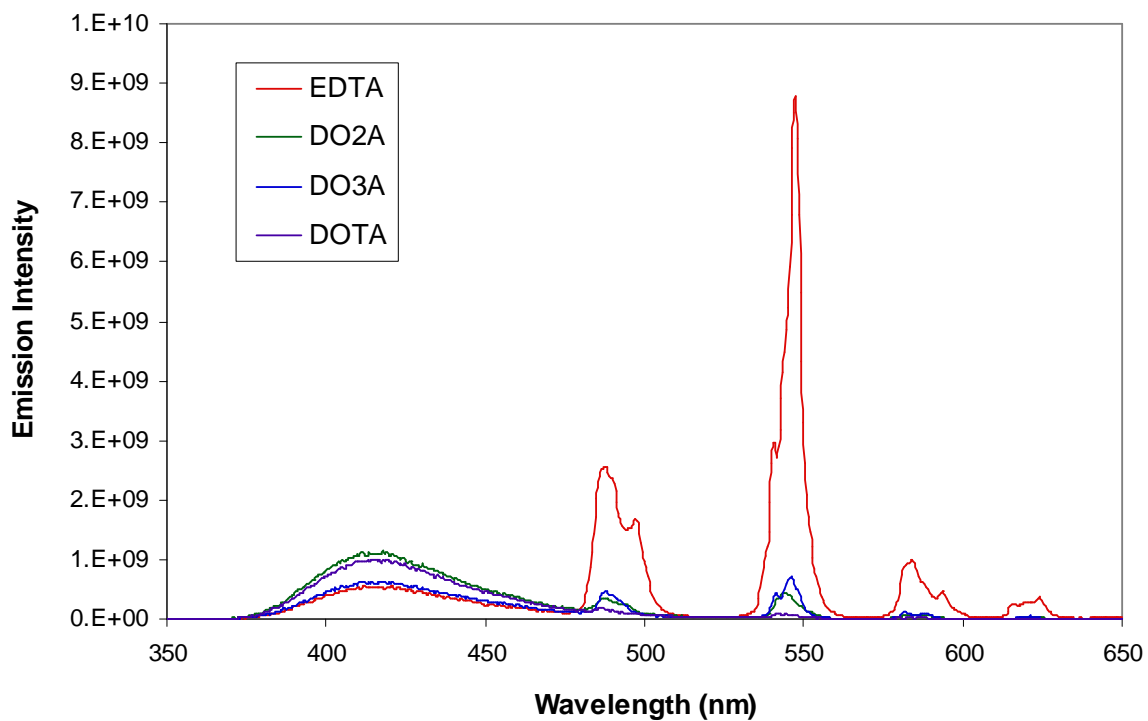
Figure 5.13. Emission spectra (λ_{ex} = 326 nm) of various Tb(ligand)(SA) complexes in 50 mM CAPS buffer, pH 12.5 (DO2A complex in CHES buffer, same concentration and pH). 10 µM SA, 1.0 mM Tb(ligand) complex. The Tb(EDTA)(SA) complex has the greatest emission intensity.

Mole fraction SA
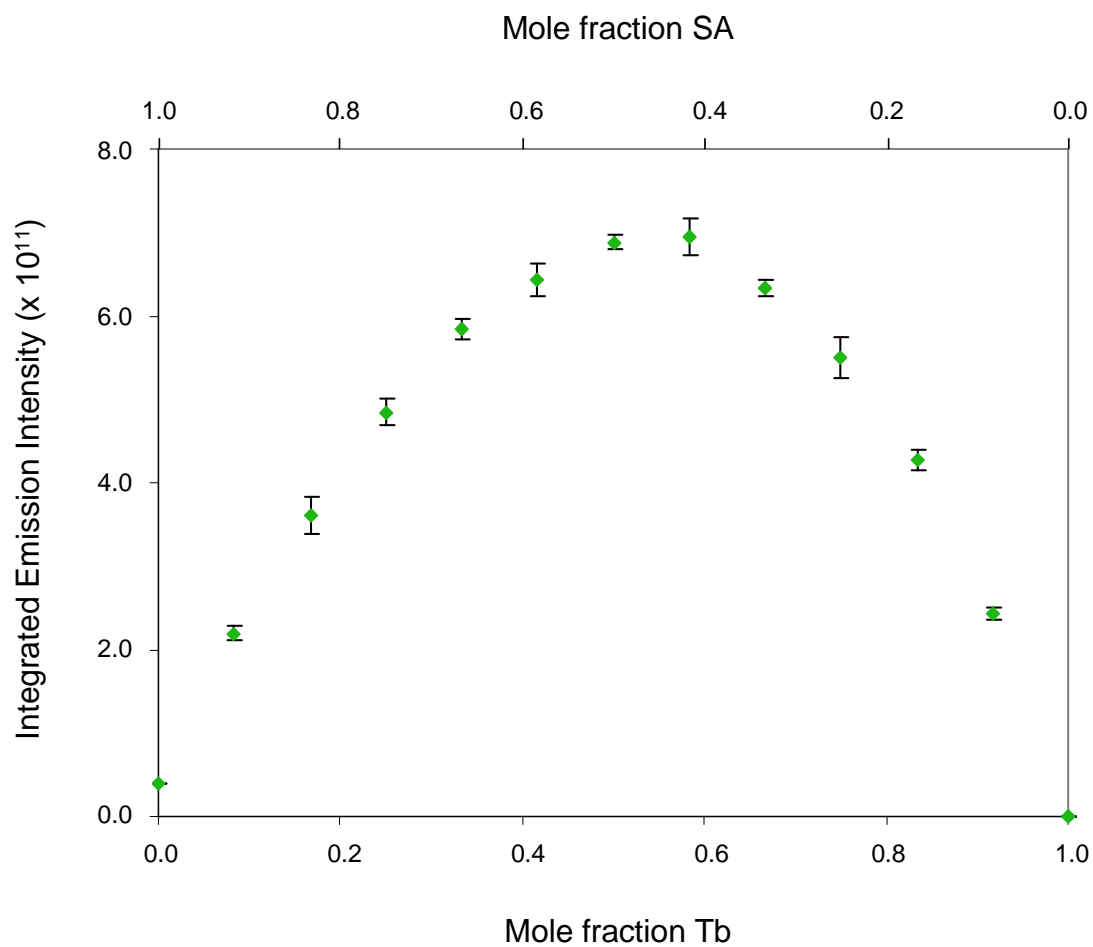
Figure 5.14. Method of continuous variations to determine binding stoichiometry of SA^{2-} to Tb(EDTA)$^{-}$. [Tb] and [SA] varied inversely from 0-120 μM in 10 μM increments with 1.00 mM EDTA in 50.0 mM CAPS buffer, pH 13.5 (λ_{ex} = 314 nm). Emission intensity integrated from 530–560 nm. Equilibration time of 24 hours.

Mole fraction SA
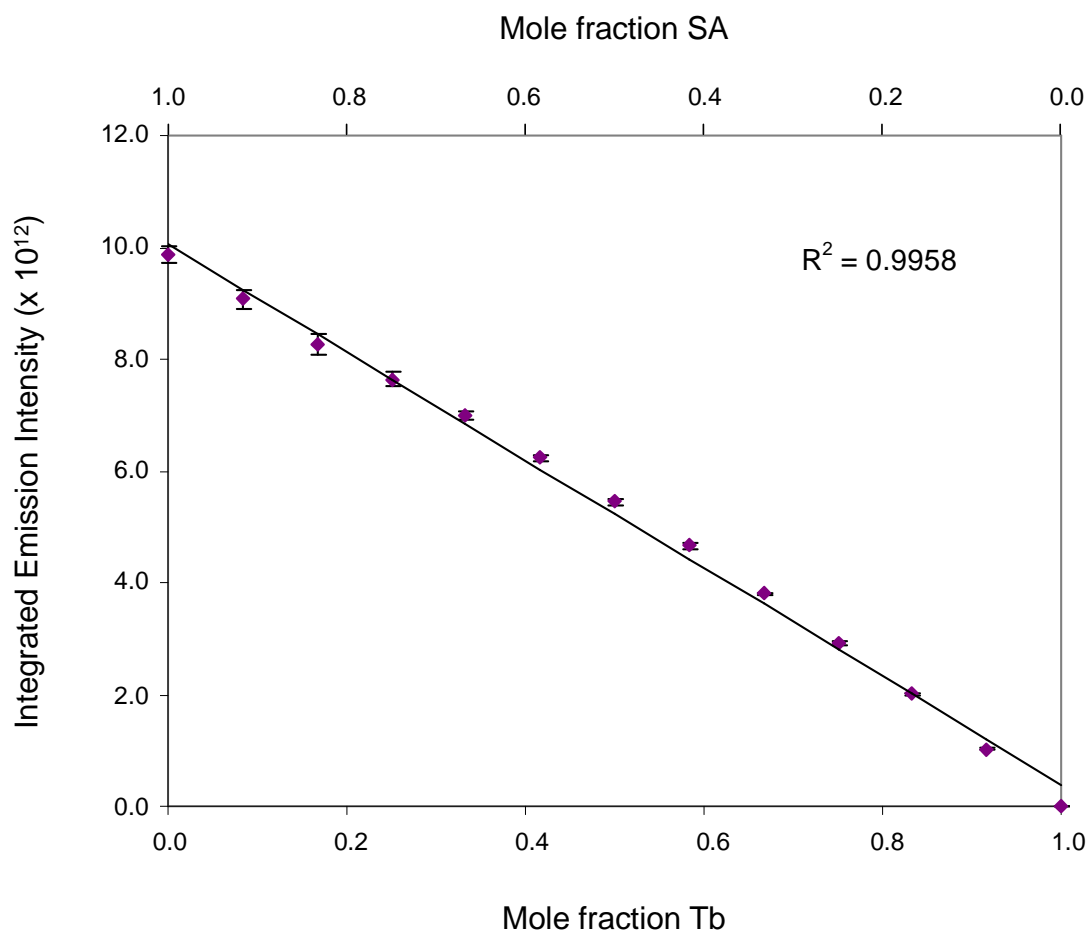
Figure 5.15. Method of continuous variations, showing linear correlation of intrinsic salicylate (SA) luminescence (419 nm) that can be used as an internal standard. Concentrations of Tb and SA were varied inversely from 0 to 120 µM in 10 µM increments, with 1.00 mM EDTA in 50 mM CAPS buffer, pH 13.5 (λ_{ex} = 314 nm). Emission intensity integrated from 375–470 nm.
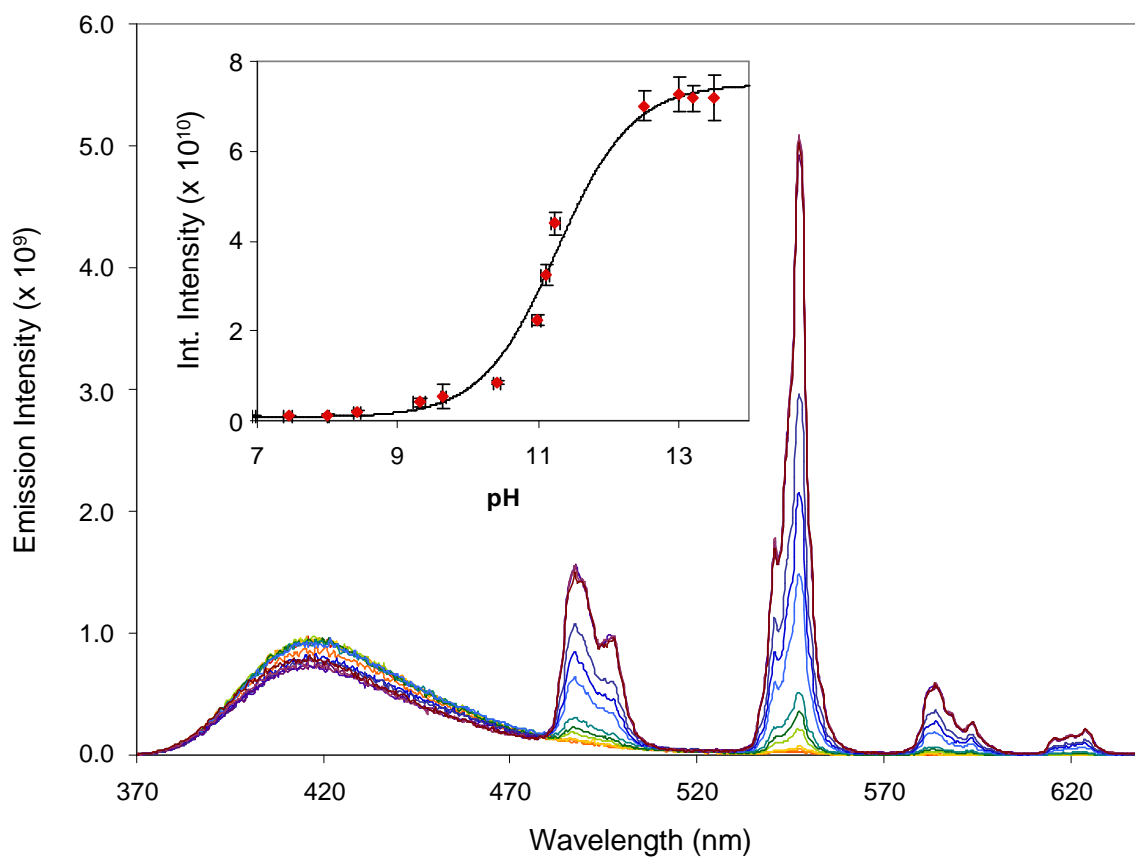
Figure 5.16. pH dependence study of 1.00 µM Tb(EDTA)(SA)$^{3-}$ in 50 mM buffer (λ_{ex} = 314 nm). [Tb(EDTA)$^-$] = 500 µM, 1 hour equilibration time. Inset: Plot of integrated emission intensity (530–560 nm) against pH.
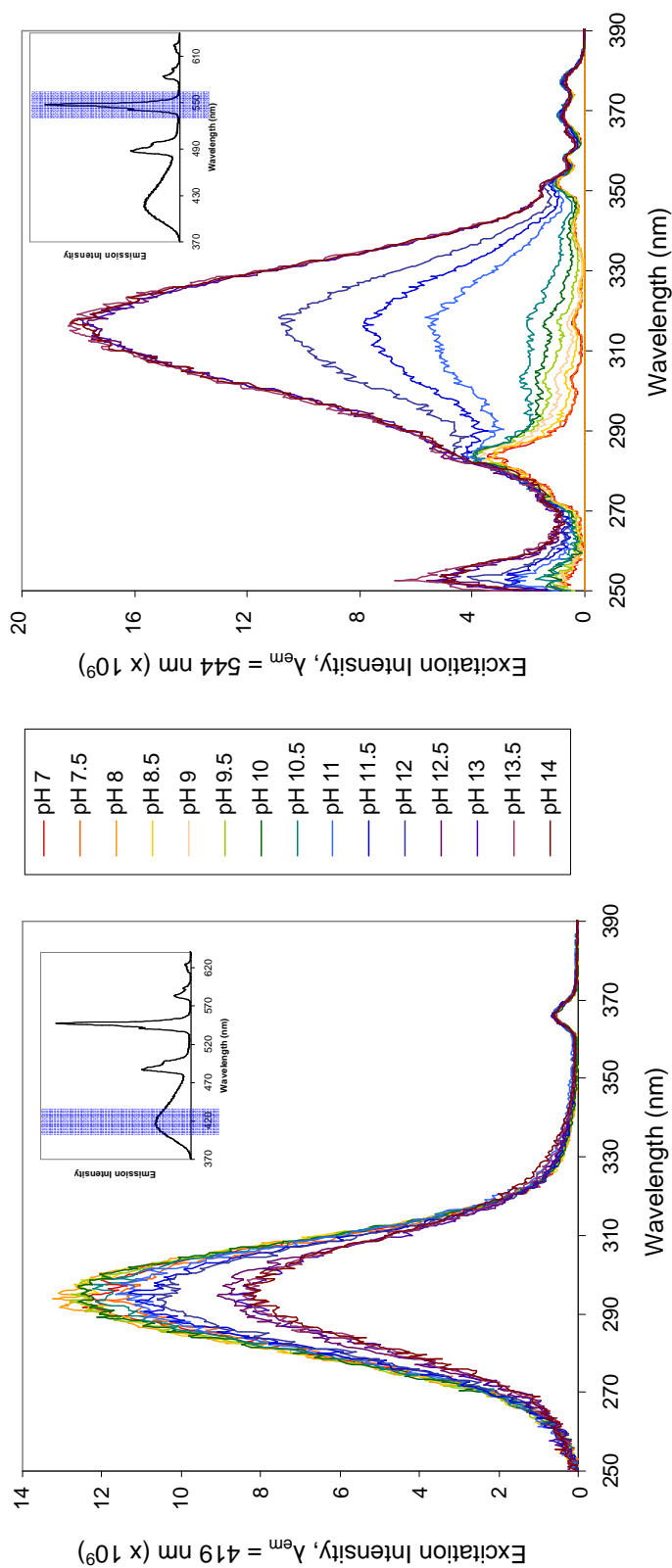
Figure 5.17. Two populations in pH dependence study of 1.00 μM Tb(EDTA)(SA)³⁻ in 50 mM buffer. [Tb(EDTA)·] = 500 μM, 1 hour equilibration time. Left: Decrease in SA⁻ population, monitored by intrinsic luminescence (λ_{em} = 419 nm) with increasing pH. Right: Increase in Tb(EDTA)(SA)³⁻ population, monitored by Tb³⁺-sensitized luminescence (λ_{em} = 544 nm).
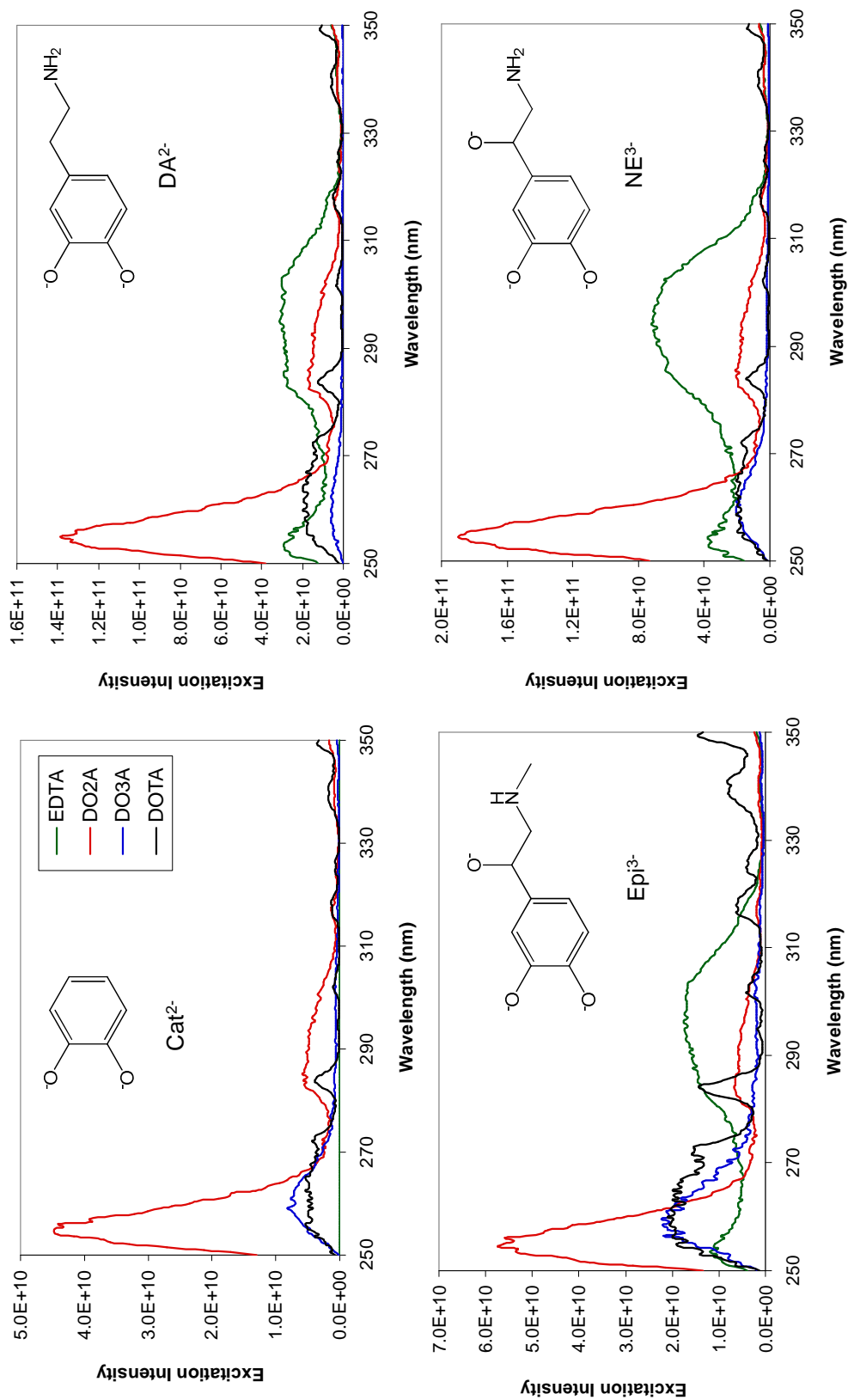
Figure 5.18. Excitation spectra (λ_{em} = 544 nm) of various Tb(ligand)(CA) complexes in 50 mM CAPS buffer, pH 13.5. 10 μM CA, 1.0 mM Tb(ligand) complex. CA abbreviations: catechol (Cat), dopamine (DA), epinephrine (Epi), norepinephrine (NE).
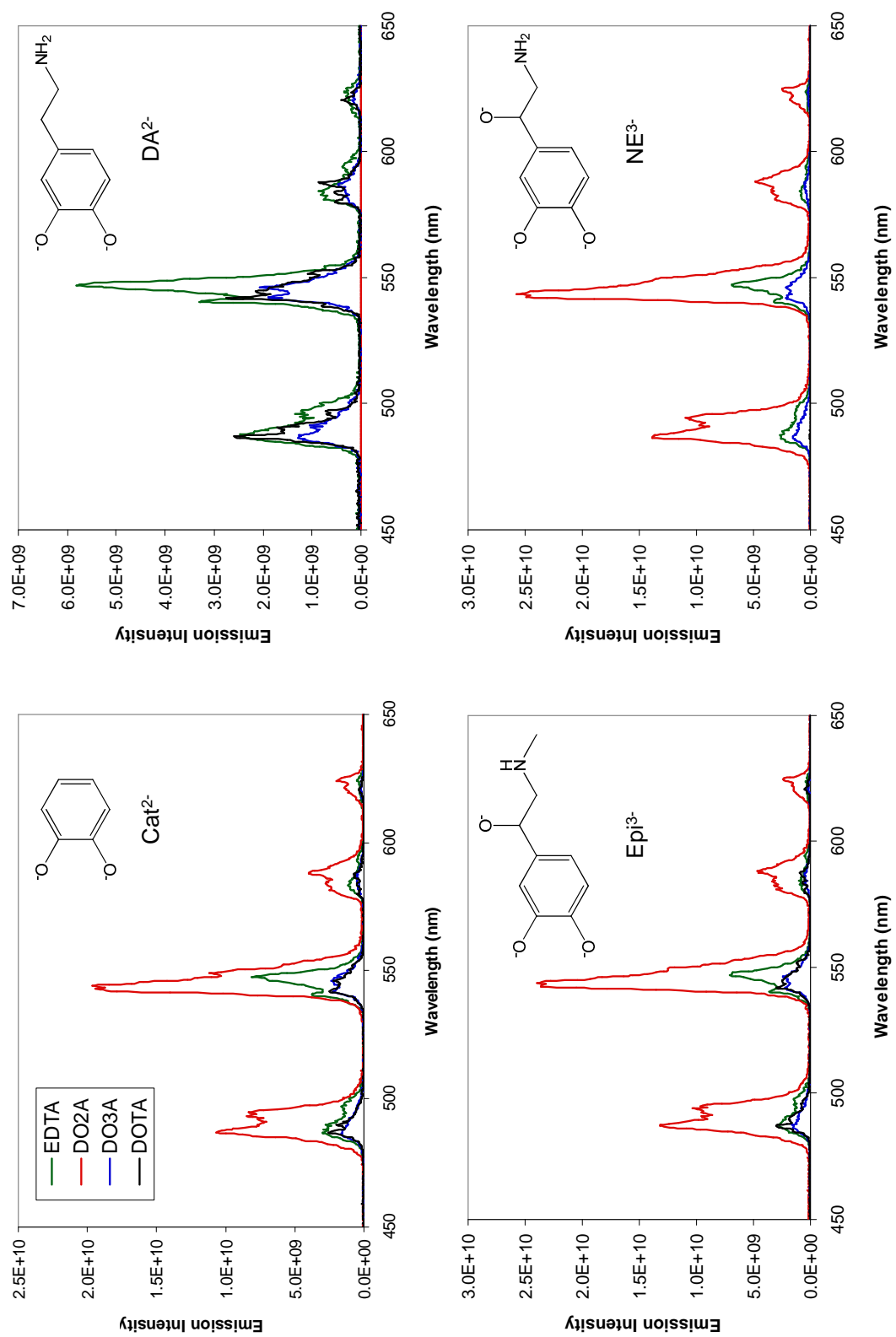
Figure 5.19. Emission spectra (λ_{ex} = 255 nm) of various Tb(ligand)(CA) complexes in 50 mM CAPS buffer, pH 13.5. 10 µM CA, 1.0 mM Tb(ligand) complex. CA abbreviations: catechol (Cat), dopamine (DA), epinephrine (Epi), norepinephrine (NE).

TABLES

Table 5.1. Protonation constants for various aromatic analytes.

Analyte	pK_{a1}	pK_{a2}	pK_{a3}	Ref
SU	3.34	7.91	-----------	23
SA	2.98	13.62	-----------	64, 65
Cat	9.48	12.08	-----------	95
Epi	8.64	9.84	13.1	94
NE	8.58	9.53	12.9	94
DA	8.89	10.41	13.1	93

SU = salicyluric acid; SA = salicylic acid; Cat = catechol;
Epi = epinephrine; NE = norepinephrine; DA = dopamine

Table 5.2. Stability constants for Tb^{3+} and Gd^{3+} with various ligands.

Type	Ligand	Coord. No.	log K_{Tb}	log K_{Gd}	Ref
Linear	EDTA	6	17.92	17.35	66
	DTPA	8	22.71	22.46	66
Cyclic	DO2A	6	---------	19.42	35
	DO3A	7	---------	21.0	67
	DOTA	8	24.8	24.6	67, 35

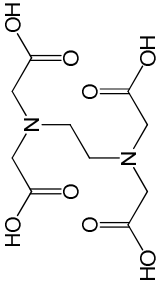Table 5.3. Protonation constants of various ligands.
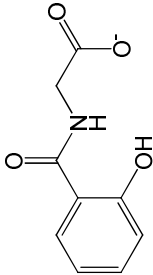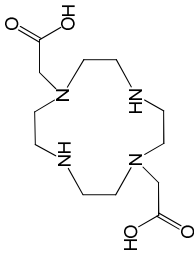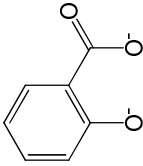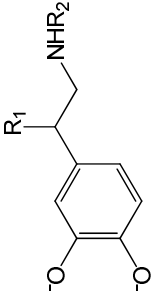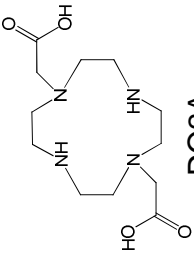
Ligand	pK_{a1}	pK_{a2}	pK_{a3}	pK_{a4}	pK_{a5}	Ref
EDTA	2.00	2.67	6.13	10.26	---------	68
DTPA	2.08	2.41	4.26	8.60	10.55	66
DO2A	2.55	3.85	9.55	10.94	---------	67
DO3A	3.39	4.40	9.51	10.72	---------	67
DOTA	4.00	4.60	9.90	11.34	---------	67

Table 5.4. Stability constants (log K) of catecholamines with various metals (25 °C, 0.2 M ionic strength).

Metal	DA	Epi	NE	Ref
Ca^{2+}	-------	5.96	5.67	91
La^{3+}	-------	5.91	-------	90
Y^{3+}	7.95	7.40	7.07	89
Al^{3+}	8.01	8.22	8.31	5

DA = dopamine; Epi = epinephrine;
NE = norepinephrine

Table 5.5. Summary of lanthanide(ligand) complexes optimized in this chapter for the detection of various analytes of biological relevance. SU = salicylurate; SA = salicylate; CA = catecholamine

Analyte	Ln³⁺	Ligand	Conditions
SU	Tb³⁺	DO2A	0.1 M TAPS, pH 8.4, λ_{ex} = 316 nm
SA	Tb³⁺	EDTA	50 mM CAPS, pH 13.5, λ_{ex} = 314 nm
CA	Tb³⁺	DO2A	50 mM CAPS, pH 13.5, λ_{ex} = 255 nm